

IDENTIFICATION AND CHARACTERIZATION OF REACTIVE
ASTROCYTES FOLLOWING OPTIC NERVE INJURY
IN ZEBRAFISH

THESIS

Presented to the Graduate Council of
Texas State University – San Marcos
in Partial Fulfillment
of the Requirements

for the Degree

Masters of SCIENCE

by

Luis D. Neve, B.S

San Marcos, Texas
December 2011

IDENTIFICATION AND CHARACTERIZATION OF REACTIVE
ASTROCYTES FOLLOWING OPTIC NERVE INJURY
IN ZEBRAFISH

Committee Members Approved:

Dana García, Chair

Joseph Koke

Shannon Weigum

Approved:

J. Michael Willoughby
Dean of the Graduate College

COPYRIGHT

by

Luis Daniel Neve

2011

FAIR USE AND AUTHOR'S PERMISSION STATEMENT

Fair Use

This work is protected by the Copyright Laws of the United States (Public Law 94-553, section 107). Consistent with fair use as defined in the Copyright Laws, brief quotations from this material are allowed with proper acknowledgment. Use of this material for financial gain without the author's express written permission is not allowed.

Duplication Permission

As the copyright holder of this work I, Luis D. Neve, authorize duplication of this work, in whole or in part, for educational or scholarly purposes only.

ACKNOWLEDGEMENTS

I would first and foremost like to express my unyielding gratitude for all of those who supported me throughout my academic career. This study could not have been completed without the intellectual guidance and encouragement of my mentor, Dr. Dana García. Her contributions were truly pivotal in the culmination of this study and the further development of my understanding of, and appreciation for, analytical biology. I would also like to thank Drs. Joseph Koke and Shannon Weigum for serving as members of my thesis committee and providing the intellectual insight and constructive criticism that allowed for the fruition of this project. I am very appreciative to Drs. Jeff Gross and Bruce Appel for providing zebrafish throughout the various stages of this study. The completion of this thesis was made possible by the technical guidance and assistance of my fellow researcher, Alissa Savage. Also, I would like to thank the entire García-Koke lab for all their contributions towards this thesis. Finally, I would like to thank both my family and my fiancé, Samantha Martinez, for their emotional support. I could have never accomplished what I have without them in my life.

This work was supported by National Science Foundation grants (IOB 0615762) to Dana García and (DBI 0821252) to both Joseph Koke and Dana García.

TABLE OF CONTENTS

	Page
ACKNOWLEDGEMENTS	v
LIST OF TABLES	vii
LIST OF FIGURES	viii
ABSTRACT	x
CHAPTER	
I. INTRODUCTION	1
II. MATERIALS AND METHODS.....	7
III. RESULTS	13
IV. DISCUSSION	29
APPENDIX.....	42
REFERENCES	46

LIST OF TABLES

Table	Page
1. Antibodies and stains used to evaluate Bysl expression following optic nerve injury in zebrafish	12

LIST OF FIGURES

Figure	Page
1. Comparison of the epitopes recognized by commercially available anti-bystin antibodies	14
2. Anti-bystin antibody labeling at various concentrations	16
3. Bysl labeling 24 hours after optic nerve lesion.....	17
4. Bysl expression is absent in the uninjured, contralateral nerve 24 hours following nerve lesion	18
5. Anti-bystin did not label astrocytes in the optic nerve of an uninjured fish	19
6. Bysl colocalizes with cytokeratin in the optic nerve of zebrafish 24 hours after nerve injury	21
7. Bysl is not expressed by oligodendrocytes in the optic nerve of zebrafish 24 hours after nerve lesion.....	22
8. Bysl positive astrocytes appear hypertrophic 24 hours after optic nerve lesion in zebrafish.....	24
9. Bysl immunoreactivity is observed within 12 hours after optic nerve lesion in zebrafish.....	25
10. Bysl does not appear to follow a diurnal pattern of expression in the optic nerve of zebrafish.....	26

11. Bysl colocalizes with Atf3 in reactive astrocytes of the optic nerve of zebrafish after nerve lesion.....	28
--	----

ABSTRACT

IDENTIFICATION AND CHARACTERIZATION OF REACTIVE ASTROCYTES FOLLOWING OPTIC NERVE INJURY IN ZEBRAFISH

by

Luis Daniel Neve, B.S.

Texas State University-San Marcos

December 2011

SUPERVISING PROFESSOR: DANA GARCIA

Following nerve injury, teleost fish are capable of initiating robust signaling cascades leading to the repair of damaged tissue and a functional recovery of nerves: a phenomenon absent in amniotes. When nerves of the CNS are injured, amniotic organisms initiate an inflammatory-like response that results in a permanent morphological change of the injured tissue, creating a collagen-rich scar around the injury site referred to as the glial scar. Reactive astrocytes are the major cellular components of the glial scar, the formation of which seems to have both a protective and inhibitory function following nerve damage in mammals. The transition of astrocytes to

a reactive state, a condition referred to as reactive gliosis, is characterized by hypertrophy and increased intermediate filament production, detected immunocytochemically by increased expression of glial fibrillary acidic protein (GFAP). However, the astrocytes in the optic nerve of zebrafish express cytokeratin, not GFAP, as their intermediate filament. Unlike GFAP expressing astrocytes, cytokeratin expression by astrocytes of the optic nerve of fish does not seem to increase in response to injury. The absence of differential intermediate filament expression in response to injury, in addition to an absence of GFAP, poses a problem when trying to identify reactive astrocytes in zebrafish. In mammals, recent studies of the protein bystin have shown it to be up-regulated during the astrocyte transition from a quiescent to a reactive state, making it a suitable marker for reactivity. A bystin-like gene (*bysl*) has been characterized in zebrafish; however, little has been shown as far as its involvement in neural tissue injury.

The goal of the study presented in this thesis was to determine if astrocytes in the optic nerve of zebrafish become reactive following nerve lesion and if reactivity could be detected via immuno-labeling of Bysl. Immunohistochemistry was performed using an anti-bystin antibody (clone S20) which recognizes an epitope with 90% homology to the predicted amino acid sequence of Bysl. Labeling with the anti-bystin antibody was observed in the cytoplasm of cytokeratin-expressing astrocytes in the optic nerve of zebrafish within 12 hours after nerve lesion. Measurements of the average nuclear size show a significant enlargement of nuclei in Bysl positive astrocytes of the injured optic nerve in comparison to astrocytes of the contralateral nerve, further suggesting anti-bystin is labeling hypertrophic reactive astrocytes. We also observed colocalization of Bysl and ATF3, a transcription factor shown to be upregulated by various stressors in the CNS, in

cells showing morphology expected for hypertrophic astrocytes, suggesting Atf3 may have a function in the reactive transition. This study is the first to show the presence of reactive astrocytes following injury in the zebrafish optic nerve, further supporting the use of zebrafish as a model organism with relevance to human health.

CHAPTER I

INTRODUCTION

Axon regeneration is essential in order to regain function after central nervous system injury. The glial cells in mammals, unlike those of fish and amphibians, do not support the growth of axons following damage of the CNS (Cohen *et al.*, 1993). Because of its accessibility, the optic nerve has become a standard model for studying regeneration of the CNS. When the optic nerve of a mouse is severed, the portions of axons on the distal end of the injury site en route to the brain begin to degenerate, a process known as Wallerian degeneration. The portions of axons on the proximal end of the lesion initially sprout neurites into the injury site. The growing neurites typically do not reach their synaptic targets, however, and most often the retinal ganglion cells die apoptotically (see García and Koke, 2009).

Glial scar formation is considered a crucial extrinsic constraint to nerve repair (Sofroniew and Vinters, 2009). The main cellular component of the glial scar are reactive astrocytes; however, oligodendrocyte precursor cells, macrophages, and meningeal cells are also typically observed (Tan *et al.*, 2004) These cells migrate into and become permanent residents of lesion sites in the CNS. The transition of

astrocytes to a reactive state, a condition referred to as reactive gliosis, entails a relatively small number of cellular divisions confined to the area surrounding a nerve lesion (Faulkner *et al.*, 2004). The reactive phenotype is characterized by hypertrophy, stellation of cytoplasmic processes, and an increase in intermediate filament production, detected immunocytochemically by increased labeling of glial fibrillary acidic protein (GFAP) and vimentin (Silver and Miller, 2004).

While it has become well established that the abundance of hypertrophic astrocytes likely serves as a physical barrier to regenerating axons, an increasing amount of evidence suggests that astrocytes also produce molecules inhibitory to neurite outgrowth. In a study performed by Rudge and Silver in 1990, hippocampal neurons were cultured on nitrocellulose membranes after the membrane had been implanted into the cerebral cortex of neonatal and adult rats for various durations of time. This allowed the researches to mimic the cellular environment of the glial scar *in vitro*. The hippocampal neurons cultured on membranes explanted from adult rats exhibited significantly less neurite outgrowth compared to those cultured on membranes explanted from neonates. This inhibition of growth on a substrate of the cellular inhabitants of the glial scar on a two dimensional surface suggests that factors in addition to mechanical inhibition restrict the ability of neurites to traverse a glial scar (Rudge and Silver, 1990). Further investigation of this observation revealed that the production of chondroitin-6-sulfate proteoglycan (CSPG) by reactive astrocytes within and around the lesion site in the adult brain contributed to the observed reduction of axonal outgrowth from hippocampal neurons (McKeon *et al.*, 1991). Investigation of CSPG expression in the zebrafish CNS after optic nerve

crush revealed no considerable upregulation in or around the injury site.

Interestingly, CSPG was detected immunohistochemically in brain nuclei of cells that do not form synapses with RGC axons, which presumably provide negative guidance information to ensure regenerating axons form synapses with their appropriate targets (Becker and Becker, 2002). Elimination of glial scar formation by preventing astrocytes from undergoing a reactive transition results in a dramatic increase in neuronal cell death surrounding CNS injury in mice (Bush *et al.*, 1999; Faulkner *et al.*, 2004; Wilhelmsson *et al.*, 2004; Li *et al.*, 2008). While the infarct size in mice with attenuated reactive astrocytes is larger than what is observed in wildtype mice, axons were able to regenerate beyond the injury site with a resulting increase in nerve function (Wilhelmsson *et al.*, 2004; Li *et al.*, 2008). These findings suggest that glial scar formation and reactive astrocytes have both a protective and inhibitory role following CNS injury. A more detailed description of the role of reactive astrocytes on axon repair is discussed in Chapter IV.

Studies have been performed using zebrafish (*Danio rerio*) as a model for axon regeneration because neurogenesis persists past the embryonic state, providing an opportunity to investigate regenerative responses to damaged neural tissue (Stenkamp, 2007). Regenerating RGC axons of zebrafish have been shown to cross an optic nerve crush site as early as 2 to 4 days after injury, growing into the optic tectum and forming terminal arborizations as early as 7 days (Bernhardt *et al.*, 1996). In a study performed by Becker *et al.*, the expression of mRNA for cell recognition molecules and neural cell adhesion molecules that promote axonal growth after a rostral and caudal spinal cord transection in zebrafish indicated that

glial reactions differ during regeneration in different regions of the CNS (Becker *et al.* 1998).

A problem arises, however, when attempting to characterize reactive astrocytes in zebrafish. Astrocytes found in the optic nerve of lower vertebrates, particularly fish, do not express GFAP as their intermediate filaments. Instead, optic nerve astrocytes of zebrafish and goldfish have been shown to express cytokeratin as their intermediate filament (Conrad *et al.*, 1998; Garcia *et al.*, 2005; Koke *et al.*, 2010). Cytokeratin expressing astrocytes have also been observed in the optic nerve of rainbow trout (Markl and Franke, 1988) and certain amphibians (Rungger-Brandle *et al.*, 1989). Unlike the case in GFAP expressing astrocytes, intermediate filament expression does not seem to increase in cytokeratin-expressing astrocytes of the optic nerve in response to injury in zebrafish (Koke *et al.*, 2010). Thus, defining the astrocytic transition to a reactive phenotype by elevated GFAP expression alone is inadequate for fish models. To properly investigate the specific macromolecules involved in the signal cascade leading to reactive astrogliosis and glial scar formation, it is imperative that the reactive phenotype of astrocytes be meticulously evaluated.

A relatively novel marker for reactivity, bystin, has been shown to correlate with traditional markers, elevated GFAP expression and hypertrophy, for reactive astrocytes in rats (Sheng *et al.*, 2004; Fang *et al.*, 2008). Bystin was first described for its role during implantation of embryos where it forms a complex with the adhesion molecules trophinin and tastin to facilitate the adhesion of trophoblast and endometrial epithelial cells at their apical cell surfaces (Suzuki *et al.*, 1999). More

recent studies have shown upregulation of bystin in astroglia after 6-hydrodopamine lesion of the nigrostriatum and stab-lesion of the cerebral cortex of adult rats. This increase in expression was not coupled with an increase trophinin expression by astrocytes, suggesting that bystin is not forming the same protein complex observed in the uterus during early embryo implantation (Sheng *et al.*, 2004). Immunodetection of bystin and GFAP following insult to the nervous system has shown bystin increases expression earlier than GFAP in rat astrocytes (Fang *et al.*, 2008). Treatment of primary cultures of astrocytes with forskolin results in an up-regulation of bystin, suggesting that expression is influenced in part by elevated intracellular cAMP levels (Sheng *et al.*, 2004). In addition, bystin expression has been shown to be more sensitive to hypoxic and ischemic condition relative to GFAP in primary cultures of mouse cerebrocortical astrocytes (Fang *et al.*, 2008). In zebrafish, a bystin-like gene (*bysl*) has been characterized; however, little has been shown as far as its involvement in neural tissue injury. In a study performed by Barresi *et al.*, mutations of the *bysl* gene led to abnormalities in optic nerve development and the phenotype or abundance of radial glia in the hindbrain, detected by highly disorganized GFAP expression by radial glia (Barresi *et al.*, 2010).

In this thesis, I report the results of my efforts to determine if astrocytes of the zebrafish optic nerve manifest a reactive phenotype in response to injury. This study was performed using antibodies raised against human bystin. These antibodies bind to an epitope with a high degree of identity to the homologous epitope of zebrafish Bysl. Bystin labeling was observed in hypertrophic cells that express cytokeratin, the intermediate filament expressed by zebrafish astrocytes in

the optic nerve. The pattern of labeling is consistent with the previously described localization of reticular astrocytes (Maggs and Scholes, 1990). This study is the first to describe the presence of reactive astrocytes in optic nerve of zebrafish following nerve lesion, supporting the use zebrafish as a model organism with relevance to human health.

CHAPTER II

MATERIALS AND METHODS

Fish Maintenance

Wild-type (AB) zebrafish were obtained from the Zebrafish International Resource Center (ZIRC) at the University of Oregon or as a gift from Dr. Jeff Gross from the University of Texas at Austin. Transgenic, Tg(*olig2:EGFP*), zebrafish were graciously donated from Dr. Bruce Appel from the Department of Pediatrics at the University of Colorado, Denver, and were subsequently bred for use in later experiments. Fish were acclimated to a 12 hour light/dark cycle for a minimum of 14 days prior to experimentation. Protocols for animal use were approved by the Texas State University-San Marcos Institutional Animal Care and Use Committee (approval # 0703_0122_07).

Experimental Design

Byst1 expression was evaluated after 90% sever of the optic nerve to observe if an upregulation of expression can be used as a marker for astrocyte reactivity in zebrafish. Protein expression was analyzed by performing immunohistochemistry using an antibody raised against bystin of human origin. To evaluate whether bystin reactivity is present in astrocytes, a colocalization study was performed using antibodies raised against human bystin and cytokeratin, the intermediate filament expressed by astrocytes in the zebrafish optic nerve. Transgenic zebrafish expressing EGFP under the control of an *olig2*

promoter were used to determine if oligodendrocytes express Bysl. Lastly, double immunolabeling experiments were performed using antibodies raised against activatingtranscription factor 3 (ATF3) and human bystin to determine if reactive astrocytes are responsible for the elevated expression of Atf3 previously reported in the optic nerve of zebrafish following nerve lesion (Saul *et al.*, 2010).

Antibody Selection

Currently, a commercially available antibody raised against zebrafish Bysl is not available. As a service provided by the technical support department of Santa Cruz Biotechnology (SCBT: Santa Cruz, CA, USA), an epitope alignment was performed in order to determine which of the commercially available antibodies raised against bystin of human origin would be best suited for use in zebrafish. While the exact epitope of the antibodies manufactured and distributed by SCBT is considered proprietary information, the company does provide an amino acid range within which the epitope of each antibody can be found. Alignment of the amino acid range of the recommended bystin antibody was performed using the BLASTp suite available online at the National Center for Biotechnology Information (<http://blast.ncbi.nlm.nih.gov/Blast.cgi?PAGE=Proteins>) as confirmation of the validity of the alignments performed by SCBT.

Optic Nerve Injury

Optic nerve injury was performed as modified from Liu and Londraville (2003) and Saul *et al.* (2010). Zebrafish were anesthetized in a 0.2% MS-222 (Finquel® tricane methanesulfonate, Argent Chemical Laboratories, Redmond, WA, USA) solution in sterile, autoclaved, tank water at subjective midday (6 hours into the light cycle). Each fish was enveloped in a paper towel wetted with sterile tank water, leaving only the head

exposed, and placed on the stage of a stereomicroscope for dissection. All surgical tools were sterilized with 70% ethanol. The left optic nerve was exposed by separating the dorsal connective tissue, cutting the lateral rectus muscle, and angling the eye rostrally in its orbit. Dumont® #5 forceps were used to sever ~90% of the optic nerve with particular care not to damage the ophthalmic artery. Any fish in which the ophthalmic artery was damaged was immediately sacrificed by overdose of MS-222 and discarded from the study. The eye was then placed back into the socket and the fish revived in aerated sterile tank water for several minutes. Once the fish regained its balance and resumed swimming normally, it was transferred to a recovery tank for the remainder of the study period. Only the left optic nerve of each zebrafish was injured, allowing for the right optic nerve to serve as an internal control.

Tissue Preparation and Cryosectioning

All fish were sacrificed by overdose in MS-222 at 24 hours after injury except as noted for analyzing the possibility of differences in *bysl* gene expression associated with diurnal rhythms. To obtain a time course of *Bysl* expression, fish were sacrificed at 3, 6, 12, 18 and 24 hours post injury. In all cases, fish were fixed in 4% formaldehyde derived by alkaline depolymerization of paraformaldehyde (PFA, Electron Microscopy Sciences, Fort Washington, PA, USA) in phosphate buffered saline (PBS) for 6 to 12 hours. The eyes, optic nerve, and brain of fixed fish were dissected intact under a stereomicroscope and washed three times for 10 minutes with PBS. To prevent ice crystal formation during cryosectioning, fixed tissues were cryoprotected using a solution of 30% sucrose in PBS for a minimum of 12 hours. The tissue was then embedded in Tissue Freezing Medium (TFM™: Triangle Biomedical Sciences, Durham, NC, USA), and frozen to a cryotome

stud oriented so that horizontal sections would include the eyes, optic nerve, and brain in a single section. Sections were cut 20 μm thick at -24°C , using either a Zeiss Microm HM 505N or Shandon cryotome and collected on gelatin coated coverslips. After collection, sections were stored at 4°C until further processing.

Immunohistochemistry

Immunohistochemistry (IHC) was performed using a protocol derived from Koke *et al.* (2010). Both indirect and direct fluorescence IHC was performed to evaluate Bysl expression following lesion to the optic nerve.

Indirect Immunohistochemistry

Sections were selected for processing based on the integrity of the optic nerve and the presence of the lesion site. A 20% non-fat dry milk solution was first pipetted onto each section to prevent non-specific binding of the antibody. After a two-hour incubation at room temperature, the blocking solution was removed, and the tissues were washed in triplicate using a solution of 0.05% Tween20 prepared in PBS (PBST). The tissue was then treated with primary antibody at an empirically derived dilution (data not shown) for either two hours at room temperature or overnight at 4°C . All primary antibodies used throughout the study were diluted in PBST. After a second round of three, 10 minute washes with PBST, a secondary antibody with a high affinity for the primary antibody was dispensed over the tissues and allowed to incubate for 2 hours at room temperature. All secondary antibodies used were diluted to empirically determined dilutions using PBST (data not shown). In order to prevent photobleaching of fluorescence, all steps after primary antibody incubation were performed under red light. After the secondary antibody reaction, the tissues were again washed three times using a PBST solution.

Hoescht DNA stain was used to label nuclei. The tissues were treated with Hoescht at a working concentration of 5 µg/ml (diluted in PBS 1:2000 from 10 mg/ml stock in water) for 20 min at room temperature. After a final round of washes, the coverslips were mounted onto microscope slides using 90% glycerol as a mounting medium. Imaging was performed using an Olympus FV1000 laser scanning confocal system and post-processing of images was performed using Adobe PhotoShop. Details of image acquisition are given in the figure legends. A list of antibodies used is presented in Table 1.

Direct Immunohistochemistry

The protocol for the direct method of immunohistochemistry is identical to that for indirect; however, the use of a fluorescently labeled antibody specific for the antigen of interest allows one to exclude the use of a secondary antibody. Consequently, all steps following treatment with a blocking solution were performed under a red light. While this method simplifies the immunolabeling procedure, the sensitivity is lower due to an absence of the signal amplification achieved when binding multiple fluorescently tagged secondary antibodies to a single primary antibody. An advantage, however, is the reduction of non-specific labeling due to secondary antibody binding to immunoglobulin-like domains found on the surface of various cell types (*Jackson Immunoresearch*, 2011).

Table 1: Antibodies and stains used to evaluate Bsl expression following optic nerve injury in zebrafish

Primary	Dilution	Secondary	Dilution
Anti-ATF3 (C-19), rabbit polyclonal, Santa Cruz Biotechnologies, Product #: SC-188	1:150 in PBST	Chicken antirabbit-IgG-AlexaFluor®647, Invitrogen, www.invitrogen.com	1:200 in PBST
Anti-bystin (S20), goat polyclonal conjugated to Texas Red, Santa Cruz Biotechnologies, Product #: SC-67526	1:50 in PBST	N/A	N/A
Anti-bystin (S20), goat polyclonal, Santa Cruz Biotechnologies, Product #: SC67526TR	1:150 in PBST	Donkey anti-goat IgG-Cy3, Abcam, http://www.abcam.com	1:150 in PBST
Anti-cytokeratin, mouse mAB anti-KRT 18, Abgent, San Diego, CA, Product #: AT2655a	1:27 in PBST	Sheep antimouse-IgG-Cy5, Abcam, http://www.abcam.com	1:400 in PBST
Nuclear stain, Hoechst, Invitrogen, Carlsbad, CA Product #: H3570	1:2000 in PBS	N/A	N/A

CHAPTER III

RESULTS

Protein Alignment Analysis

Amino acid sequence alignment of bystin from human and Bysl of zebrafish origin shows 84% homology between the two proteins overall. Currently, there are seven different clones of antibody raised against bystin of human origin commercially available from Santa Cruz Biotechnology. When the epitopes of these antibodies were aligned to zebrafish Bysl, the epitope of the anti-bystin clone S20 antibody showed a 90% homology between zebrafish and human bystin (per technical representative, Santa Cruz biotechnology). While the exact epitope of the antibodies manufactured and distributed by SCBT is considered proprietary information, the company does provide an amino acid range which includes the epitope of each antibody. For the anti-bystin (S20) antibody, the range provided was from amino acid 300-350 of the 437 amino acid sequence of human bystin. This amino acid sequence was aligned to the protein sequence of zebrafish Bysl to confirm the validity of the alignment performed by the technicians at SCBT. This alignment revealed a 82% identity with a 92% homology based on the presence of conservative substitutions to amino acids 283-333 of the 422 amino acid sequence of zebrafish Bysl (Figure 1).

Clone 19; Range: 215-223			
Identities = 7/9 (78%), Positives = 8/9 (89%), Gaps = 0/9 (0%)			
215	QILYVTEPE	223	
	Q+LY_TEPE		
198	QVLYLTEPE	206	
S-20, C-19; Range: 350-400			
Identities = 42/51 (82%), Positives = 47/51 (92%), Gaps = 0/51 (0%)			
350	YALPYRVLDALVFHFLGFRTEKREL	PVLWHQCLLTLVQRYKADLATDQKEA	400
	YALP+RVLDALV_HFL_FRT+KR_LPVLWHQ_LLTLVQRYKADL+++QKEA		
333	YALPFRVLDALVAHFLSFRTDKRILPVLWHQSLLTLVQRYKADLSSEQKEA	383	
Q17; Range: 150-200			
Identities = 42/51 (82%), Positives = 47/51 (92%), Gaps = 0/51 (0%)			
150	IIMEKLTEKQTEVETVMSEVSGFMPQLDPRVLEVYRGVREVL	SKYRSGKL	200
	IIMEK+TEKQTEV_TV+SEVSG__MPQ+DPRV+EYRGV_+VLSKYRSGKL		
176	IIMEKITEKQTEVGTVLSEVSGHAMPQMDPRVVEYRGVSKVL	SKYRSGKL	226
A-10, G-1, H-300; Range: 138-437			
Identities = 251/295 (85%), Positives = 277/295 (94%), Gaps = 0/295 (0%)			
138	NKNPPARRTLADIIMEKLTEKQTEVETVMSEVSGFMPQLDPRVLEVYRGVREVL	SKYRS	197
	+KNPP_RRTLADIIMEK+TEKQTEV_TV+SEVSG__MPQ+DPRV+EYRGV_+VLSKYRS		
121	SKNPPMRRTLADIIMEKITEKQTEVGTVLSEVSGHAMPQMDPRVVEYRGVSKVL	SKYRS	180
198	GKLPKAFKIIPALSNWEQILYVTEPEAWTAAAMYQATRIFASNLKERMAQRFYNL	VLLPR	257
	GKLPKAFKIIPALSNWEQ+LY+TEPE_W+AAAMYQATRIF+SNLKERMAQRFYNL	VLLPR	
181	GKLPKAFKIIPALSNWEQVLYLTEPETWSAAAMYQATRIFSSNLKERMAQRFYNL	VLLPR	240
258	VRDDVAEYKRLNFHLYMALKKALFKPGAWFKGILIPLCESGCTLR	EAIIVGSIITKCSI	317
	+RDD+AEYKRLNFHLY_ALKKALFKP_AWFKGIL+PLCESG+CTLR	EAIIVGSIITKCSI	
241	IRDDIAEYKRLNFHLYSALKKALFKPAWFKGILLPLCESGCTLR	EAIIVGSIITKCSI	300
318	PVLHSSAAMLKIAEMEYSGANSIFLRLLLDKKYALPYRVLDALVFHFLGFRTEKREL	PVL	377
	PVLHSSAAMLK+AEMEY+GANSIFLRL+LDKKYALP+RVLDALV_HFL_FRT+KR_LPVL		
301	PVLHSSAAMLKLAEMEYNGANSIFLRLMLDKKYALPFRVLDALVAHFLSFRTDKRILPVL	360	
378	WHQCLLTLVQRYKADLATDQKEALLELLRLQHPQLSPEIRRELQSAVPRDVEDV	432	
	WHQ_LLTLVQRYKADL+++QKEALLELL__HPQ+S_EIRRELQSA_PRD+ED_		
361	WHQSLLTLVQRYKADLSSEQKEALLELLKAHTHPQISSEIRRELQSAEPRDLEDA	415	

Figure 1: Comparison of the epitopes recognized by commercially available anti-bystin antibodies. Seven clones of antibodies raised against bystin of human origin are commercially available by Santa Cruz Biotechnology (Clone 19, S-20, C-19, Q-17, A-10, G-1, and H-300). While the exact epitope recognized by each antibody is retained by SCBT, the amino acid range in which the epitope of each clone is found was aligned to zebrafish Bysl. The amino acid sequence of human bystin appears as red text. Antibodies were ranked in increasing order according to the percent positive identity. Due to the large amino acid range provided by SCBT, clones A-10, G-1, and H-300 were not considered potential candidates for use in zebrafish. While clones S-20, C-19, and Q-17 all had the same percent homology, the technicians at SCBT stated that the exact epitope recognized by clone S-20 had the highest level of identity to the homologous epitope of zebrafish Bysl. The anti-bystin S20 antibody was chosen as the best candidate to test for bystin expression after optic nerve lesion in zebrafish.

Bysl Expression following Optic Nerve Injury

Immunohistochemistry was performed using a dilution range from 4 µg/ml (1:50 dilution of 200 µg/ml stock) to 1 µg/ml (1:200) to determine the optimum working concentration of anti-bystin (S20) antibody for labeling zebrafish Bysl. This range was chosen based on the recommended working concentration range provided by SCBT for detection of bystin in rat, mice, and humans. Nucleated cells were labeled along the periphery of fascicles of the optic nerve using concentrations of 4 µg/ml (1:50), 2 µg/ml (1:100), and 1.3 µg/ml (1:150) 24 h after nerve lesion (Figure 2). Because of the degree of labeling and the absence of evidence to suggest a high degree non-specific antigen recognition (Figure 15), the 1:50 dilution was deemed the best of the concentrations analyzed and was used as the working concentration for the remainder of the study.

Bysl was detected in the cytoplasm of nucleated cells with morphological characteristics suggestive of astrocytes along the periphery of fascicles of the injured (left) optic nerve 24 hours after nerve lesion (Figure 3). This labeling was not observed in the contralateral (right) nerve of the same tissue section (Figure 4) or the left nerve of an uninjured fish sacrificed at the same time point (Figure 5). Labeling was also observed to trail into the interior of fascicles of injured nerves, presumably in the cytoplasmic processes of the same cell type inhabiting the periphery. The pattern of labeling observed is consistent with both the location and morphology of reticular astrocytes in the optic nerve of zebrafish described by Maggs and Scholes (1990).

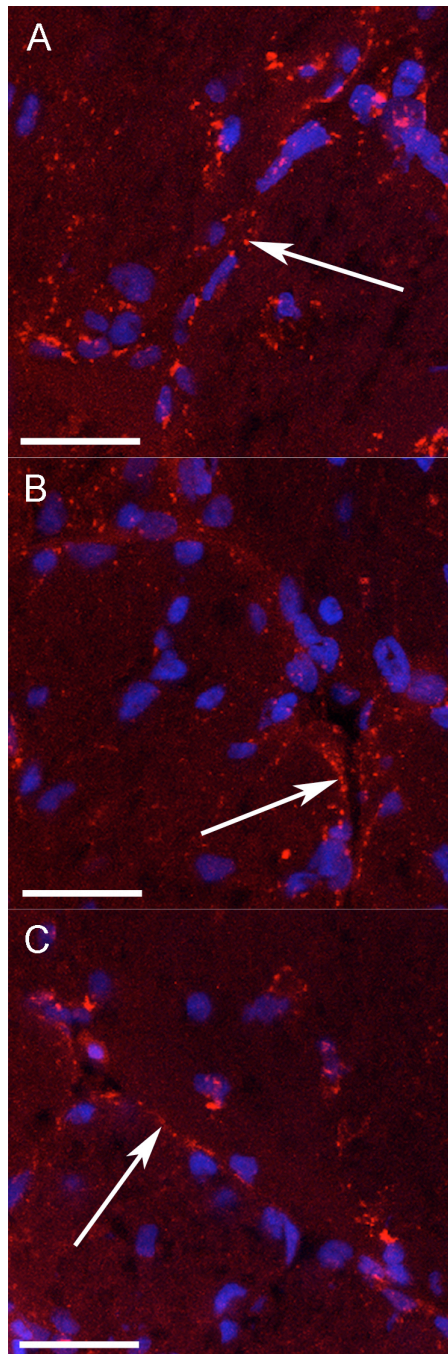


Figure 2: Anti-bystin antibody labeling at various concentrations. Each image presented is a z-projection of 20 optical sections 0.5 μm thick obtained using a 60x oil-immersion objective (NA 1.4). Hoescht stained nuclei appear blue in all images. Bysl labeling appears red in each image. Antibody was applied at a concentration of 4 $\mu\text{g}/\text{ml}$ (A), 2 $\mu\text{g}/\text{ml}$ (B), and 1.3 $\mu\text{g}/\text{ml}$ (C). The arrows in this figure are identifying the borders of fascicles in the zebrafish optic nerve. The 4 $\mu\text{g}/\text{ml}$ concentration was deemed the best of the concentrations analyzed and was used as the working concentration for the remainder of the study. Scale bars represent 20 μm in each image.

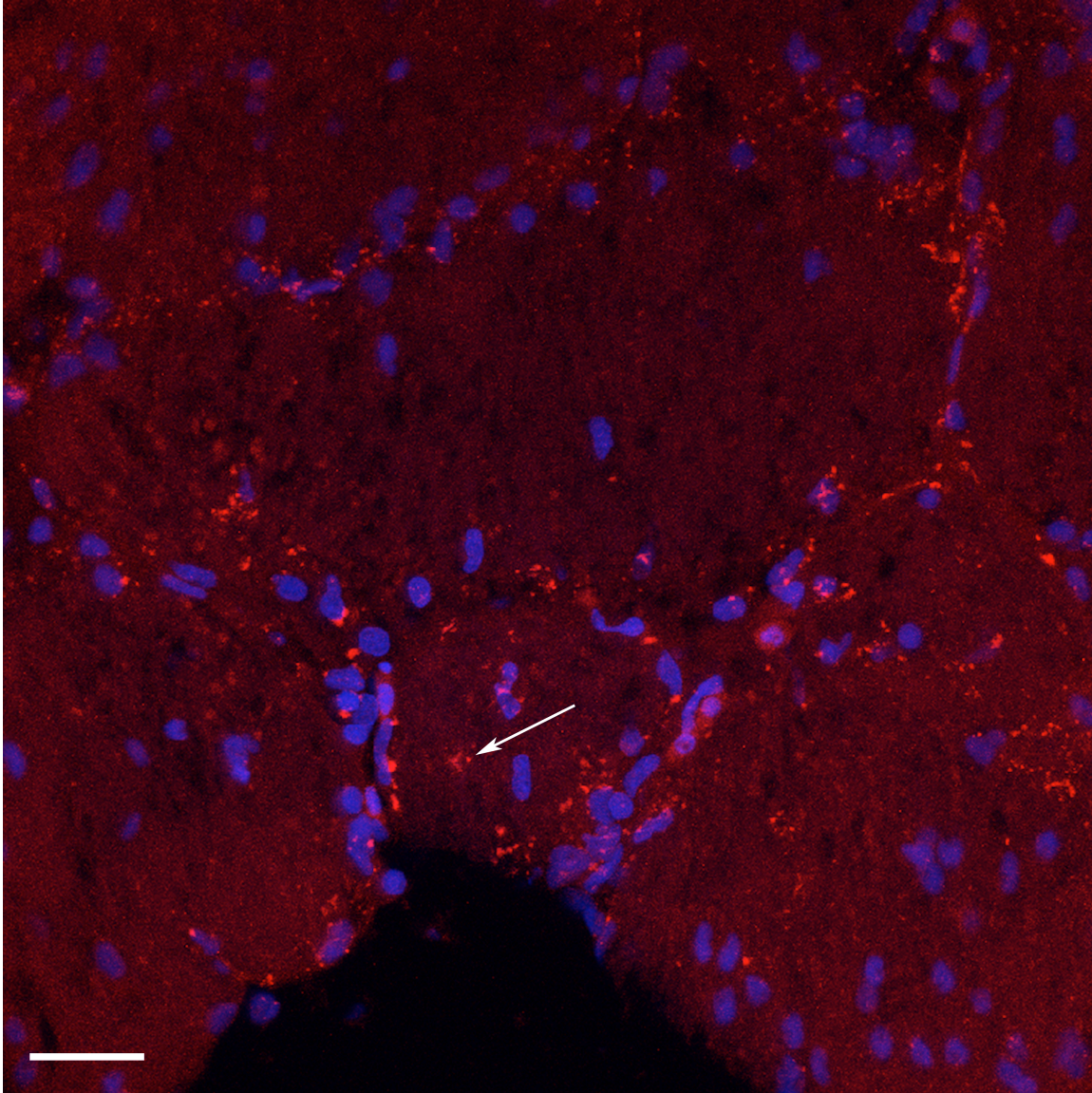


Figure 3: Bysl labeling 24 hours after optic nerve lesion. Confocal image of the injured (left) optic nerve of a zebrafish sacrificed 24 hours post injury. This image is a z-projection of 20 optical sections each 0.5 μm thick obtained using a 60x oil immersion objective with a numerical aperture of 1.4. Red shows the localization of anti-bystin labeling. Nuclei appear blue in this image, identified using a Hoescht DNA stain. Bysl labeling along the periphery of fascicles in the optic nerve is consistent with the location of reticular astrocytes in the optic nerve of zebrafish (Maggs and Scholes, 1990). The arrow is showing Bysl labeling in the interior of a fascicle of the optic nerve, believed to be in a cytoplasmic process of an astrocyte inhabiting the periphery of the fascicle. The scale bar represents 20 μm .

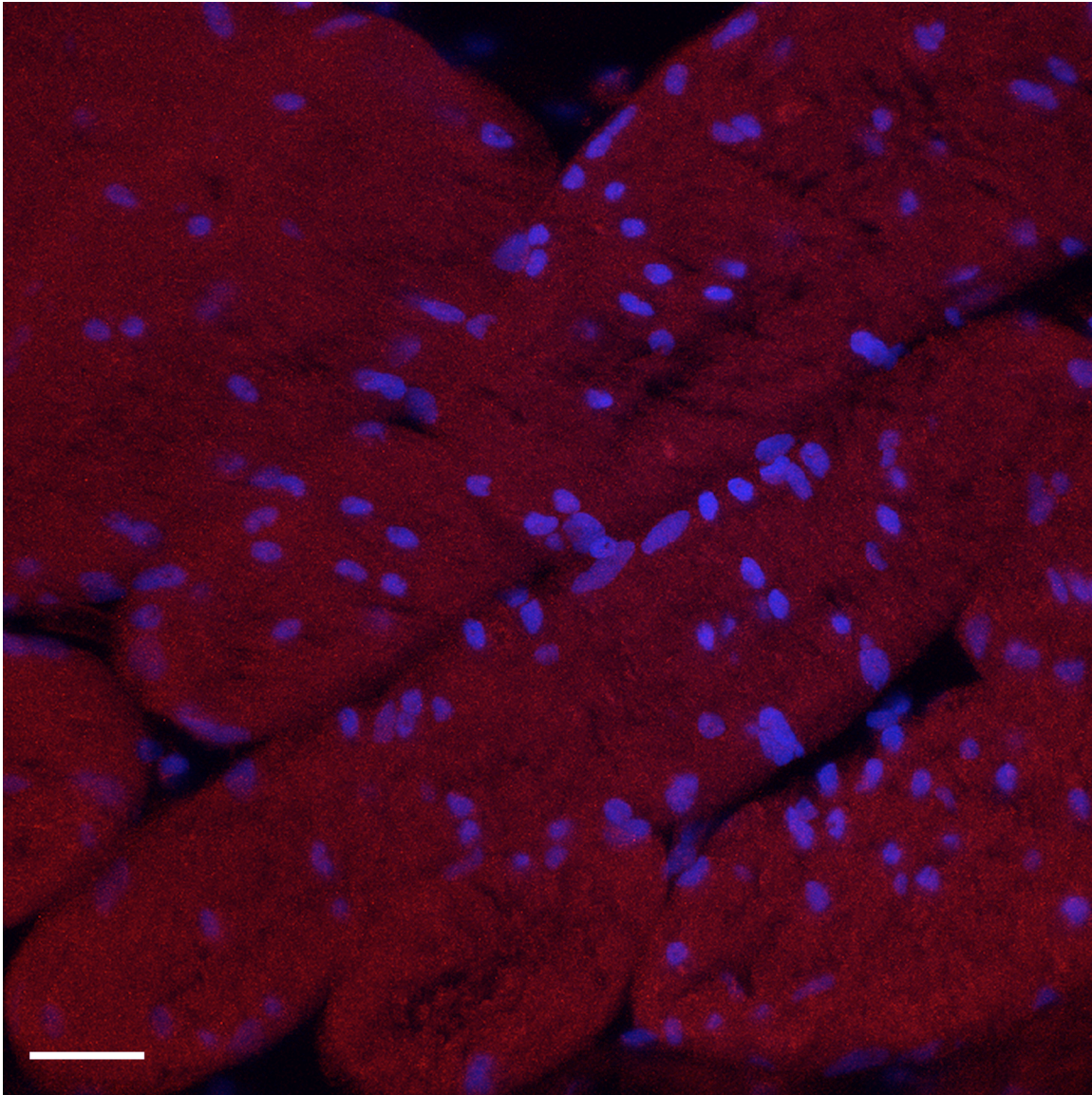


Figure 4: Bysl expression is absent in the uninjured, contralateral nerve 24 hours following nerve lesion. Confocal image of the contralateral, uninjured (right) optic nerve of a zebrafish sacrificed 24 hours post injury. This image is a z-projection of 20 optical sections each 0.5 μm thick obtained using a 60x oil immersion objective (NA 1.4). Nuclei appear blue in this image. Bysl expression, observed as discrete, localized areas of red labeling in the left optic nerve, was not detected in any nucleated cells in the right optic nerve 24 hours after nerve injury. This difference in labeling between the injured and uninjured nerve suggests Bysl is being expressed by astrocytes as a result of nerve insult, a possible indication that labeled cells may be reactive astrocytes. The scale bar in this image represents 20 μm.

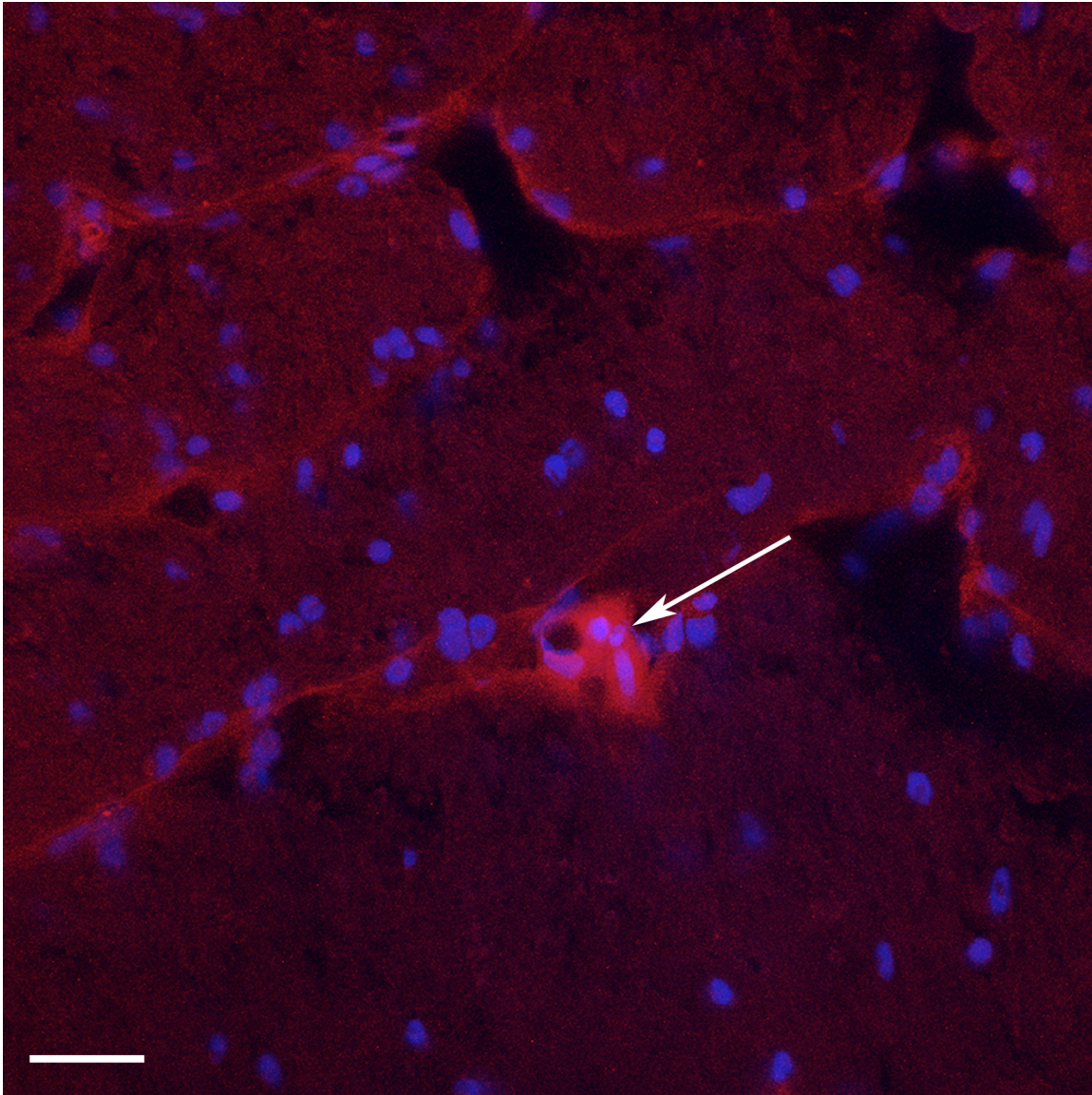


Figure 5: Anti-bystin did not label astrocytes in the optic nerve of an uninjured fish. Confocal image of the left optic nerve of a normal, uninjured zebrafish sacrificed at the same midday time point as 24 hour injured fish. This image is a z-projection of 20 optical sections each 0.5 μm thick obtained using a 60x oil immersion objective (NA 1.4). Anti-bystin antibodies did not label any nucleated cells in either the left or right optic nerve of normal fish. The arrow is pointing to auto-fluorescent cells of unknown origin. Auto-fluorescence was determined by switching between various monochromatic filter cubes using the epifluorescent capability of an Olympus FV-1000 confocal microscope. The scale bar in this image represents 20 μm .

The astrocytes of the optic nerve of zebrafish and other lower vertebrates express cytokeratin rather than GFAP as their intermediate filaments (Markl and Franke, 1988; Rungger-Brandle *et al.*, 1989; Conrad *et al.*, 1998). In order to determine if the Bysl positive cells observed in the injured optic nerve of zebrafish were astrocytes, a double immunolabeling experiment was performed using anti-cytokeratin and anti-bystin antibodies. Cytokeratin labeling was observed in the cytoplasm of cells in both the injured and contralateral nerves in the same tissue section. Consistent with previously reported data, the degree or intensity of cytokeratin labeling appeared the same in both the injured and the contralateral nerves (Koke *et al.*, 2010). Every Bysl positive cell appeared to express cytokeratin in the injured nerve 24 hours after injury, further suggesting that these cells are indeed astrocytes (Figure 6). Cytokeratin did, however, label cells in the injured nerve with no detectable Bysl expression.

Oligodendrocyte precursor cells have been demonstrated to invade the glial scar following nerve lesion (Levine *et al.*, 2001). To evaluate whether oligodendrocytes also express Bysl in response to injury, immunohistochemistry was performed using anti-bystin antibodies in transgenic zebrafish that express *egfp* under an *olig2* promoter. The transcription factor Olig2 has been shown to promote oligodendrocyte differentiation and is expressed in both oligodendrocyte precursor cells and mature oligodendrocytes (Zhou *et al.*, 2001). Bysl labeling did not colocalize with *egfp* expression, indicating that oligodendrocytes do not express Bysl, even in response to injury (Figure 7).

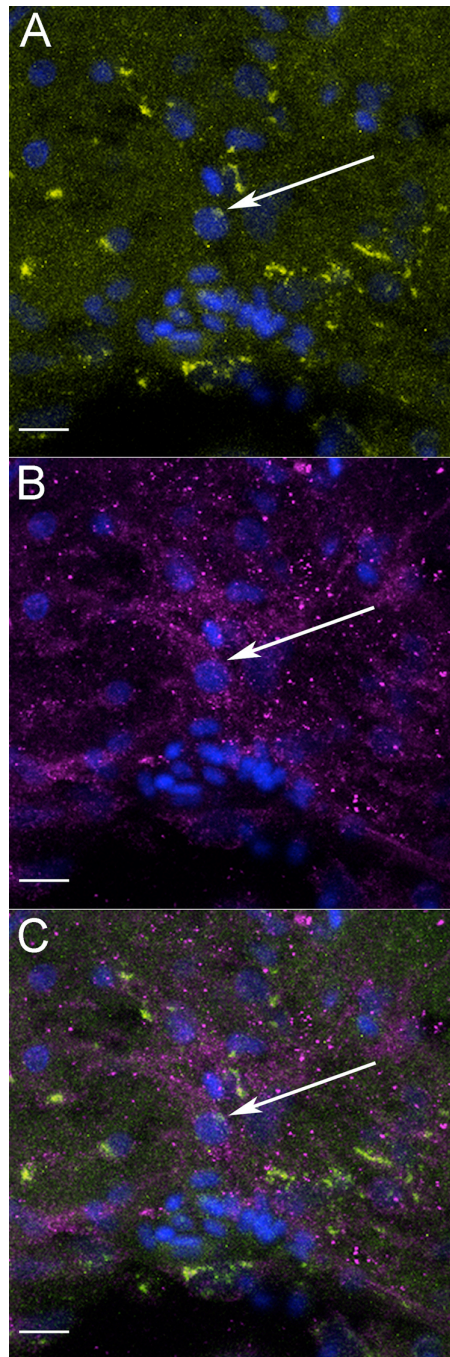


Figure 6: Bysl colocalizes with cytokeratin in the optic nerve of zebrafish 24 hours after nerve injury. Confocal images of zebrafish optic nerve obtained 24 hours post-injury. Each image is a z-projection of 20 optical sections (each 0.5 μm thick) obtained using a 60x oil-immersion objective (NA 1.4). Nuclei appear blue in all images. A, B, and C are identical and show an example of an optic nerve astrocyte (arrow). In A, yellow represents Bysl labeling; in B, magenta indicates anti-cytokeratin, and C is A and B merged. The colocalization of Bysl with cytokeratin suggests the anti-bystin antibody is indeed labeling astrocytes in the zebrafish optic nerve following nerve lesion. Scale bars in each image represent 10 μm .

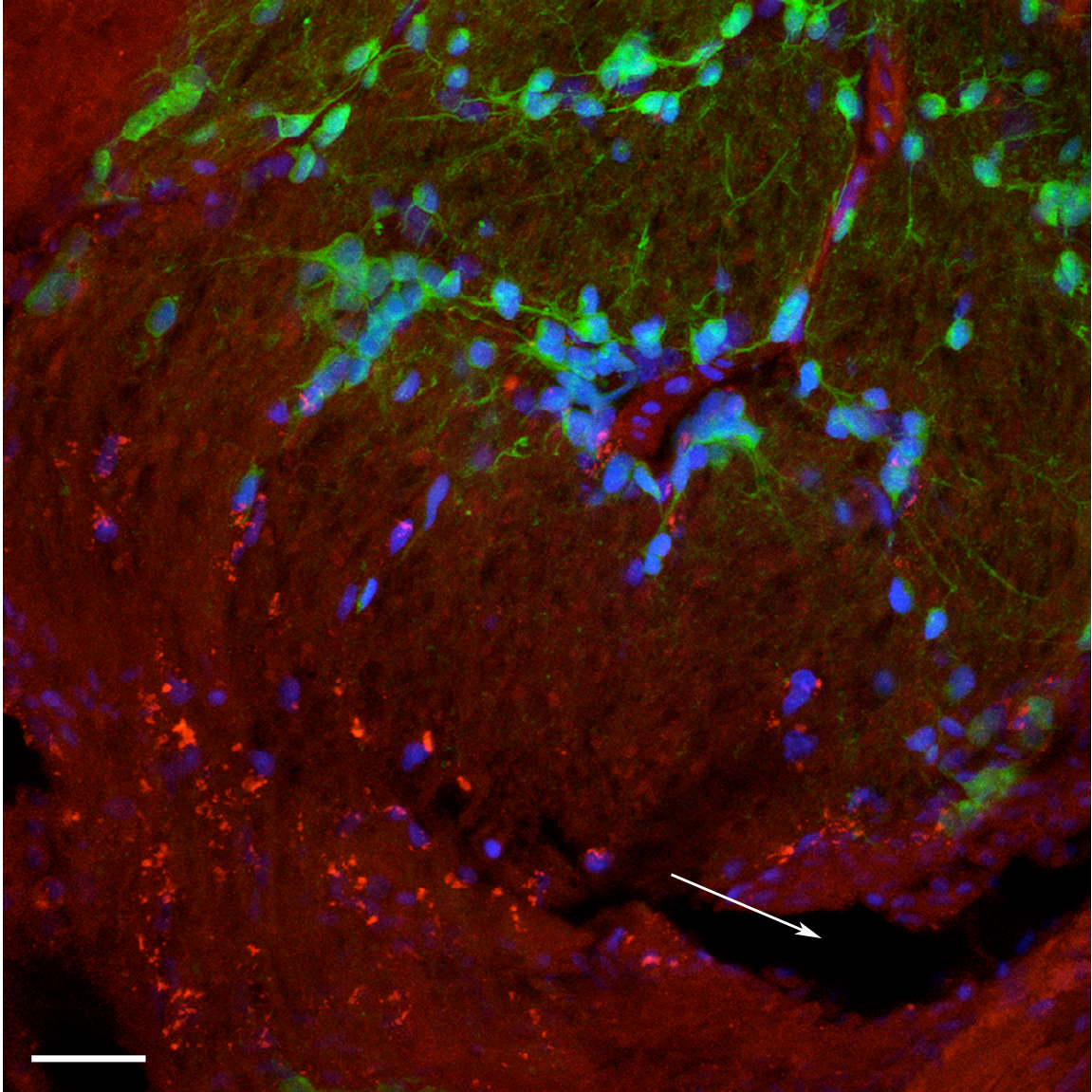


Figure 7: Bysl is not expressed by oligodendrocytes in the optic nerve of zebrafish 24 hours after nerve lesion. Confocal image of an injured optic nerve of a transgenic *olig2:efgp* zebrafish 24 hours after nerve lesion. This image is a z-projection of 20 optical sections each 0.5 μm thick obtained using a 60x oil immersion objective with a numerical aperture of 1.4. Nuclei appear blue in this image, identified by treatment with Hoescht DNA stain. Bysl labeling appears red in this image. Green represents oligodendrocytes identified by *efgp* expression under control of an *olig2* promoter. Bysl labeling did not colocalize with EGFP, indicating that oligodendrocytes do not express Bysl in response to injury. An interesting observation is the absence of EGFP in oligodendrocytes in the immediate area surrounding the nerve lesion (arrow). Scale bar represent 20 μm in this image.

Distinguishing characteristics of reactive astrocytes include hypertrophy and hyperplasia, as well as an enlargement of the nucleus (Pekny *et al.*, 2007). To further investigate whether the astrocytes expressing Bysl were reactive, the nuclear size of astrocytes of the injured and contralateral optic nerves were compared. Astrocyte nuclei were identified by anti-bystin labeling in the injured optic nerve. Since there was no detectable Bysl expression in the contralateral nerve, astrocytes' nuclei were determined by morphological characteristics and localization. The average area of astrocyte nuclei in the injured optic nerve was $40 \mu\text{m}^2 \pm 10 \mu\text{m}^2$ (SD; $n = 20$), and the average area of astrocyte nuclei from the contralateral, uninjured nerve was $25 \mu\text{m}^2 \pm 9 \mu\text{m}^2$ (SD; $n = 20$). A student's T-test revealed that this difference was highly significant ($P < 0.01$), suggesting that Bysl is being expressed by hypertrophic astrocytes in the injured optic nerve (Figure 8).

Anti-bystin labeling was also analyzed in fish sacrificed at 3, 6, 12, and 18 hours after optic nerve lesion to determine the time course of expression. Labeling was not apparent at 3 or 6 hours after injury (Figure 9). Elevated Bysl expression was evident within 12 hours after injury; however, it was only observed in one out of five sections examined (representing two fish). More consistent labeling was observed in sections taken from fish killed 18 hours after nerve lesion. Visual analysis suggests a gradual progression in the number of cells labeled with anti-bystin from 12 to 24 hours, with 24 hours having the highest number of Bysl positive cells (Figure 9). In order to eliminate the possibility of a diurnal pattern of expression, anti-bystin labeling was also analyzed in normal (uninjured) fish sacrificed at the same 12, 18, and 24 hour time points of optic

nerve injured fish. There was no detectable Bysl expression observed in uninjured fish analyzed at any time point (Figure 10).

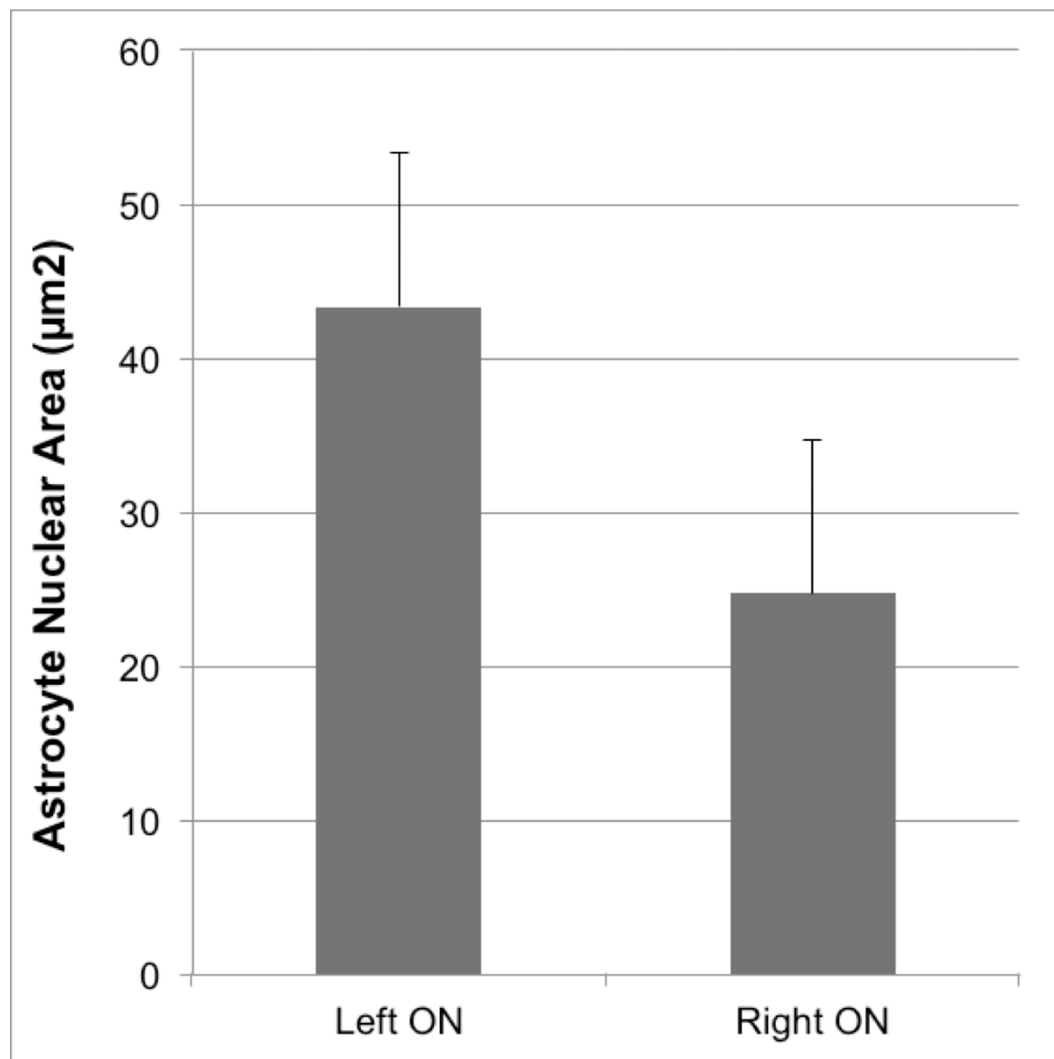


Figure 8: Bysl positive astrocytes appear hypertrophic 24 hours after optic nerve lesion in zebrafish. The astrocytes' nuclear sizes were compared between the left and right optic nerve 24 hours after nerve lesion. The area of 20 nuclei were obtained from z-projection of 13 optical slices (0.35 µm each), representing a total thickness of 4.55 µm. Astrocytes of the injured optic nerve were identified by Bysl immunoreactivity. A student's T-test revealed that the difference between astrocyte nuclei from the injured (left) and uninjured (right) nerves was highly significant ($P < 0.01$), suggesting that Bysl is being expressed by hypertrophic astrocytes in the injured optic nerve.

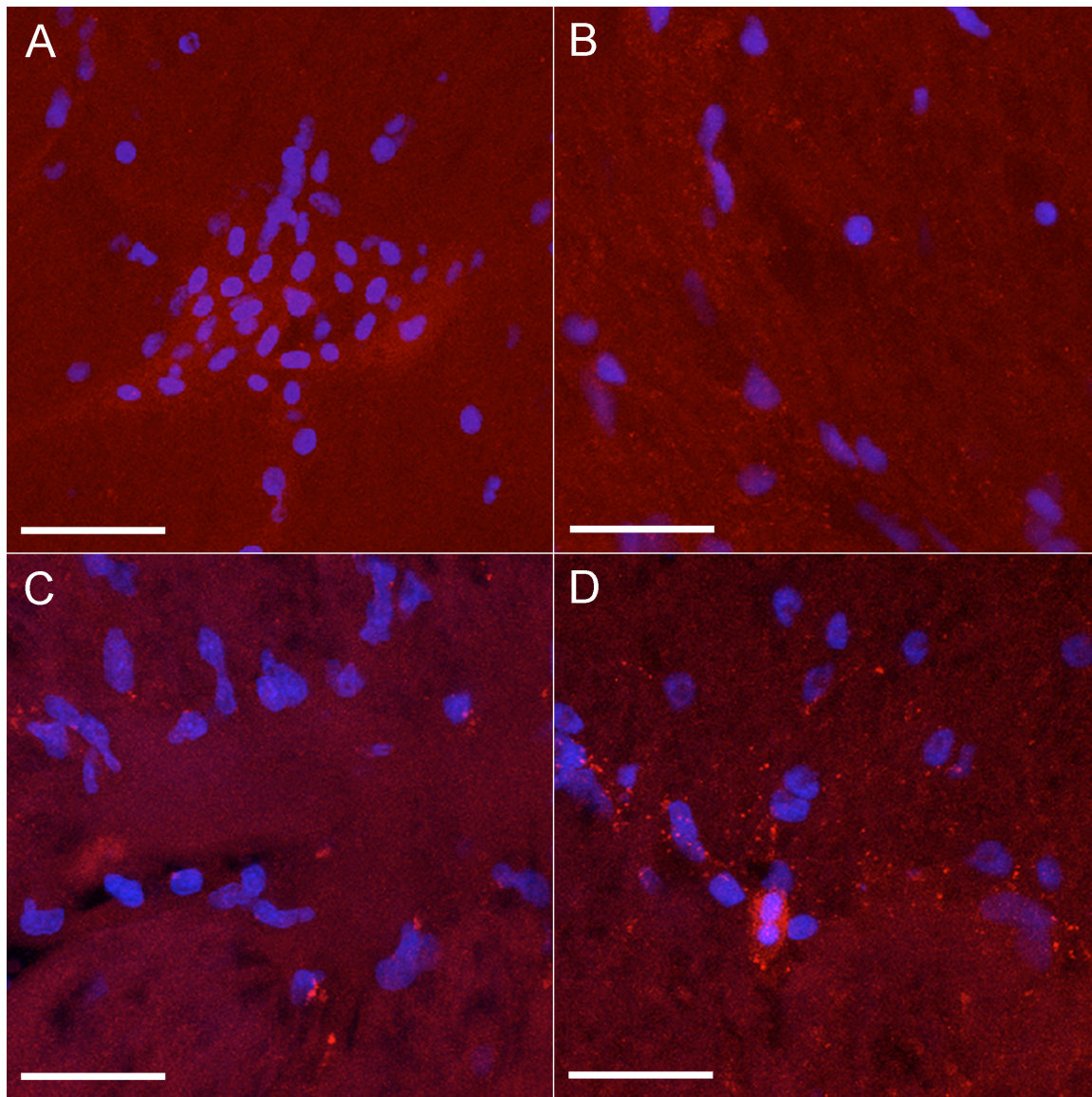


Figure 9: Bysl immunoreactivity is observed within 12 hours after optic nerve lesion in zebrafish. Confocal images of an injured optic nerve from zebrafish sacrificed at (A) 3 hours, (B) 6 hours, (C) 12 hours and (D) 18 hours post-injury. Each image presented is a z-projection of 20 optical sections 0.5 μm thick obtained using a 60x oil-immersion objective with a numerical aperture of 1.4. Nuclei appear blue in all images. Red shows the localization of Bysl determined by direct immunofluorescence in optic nerve astrocytes. Bysl expression was first observed 12 hours following nerve lesion (C). There is gradual progression in the number of cells labeled with anti-bystin from 12 to 24 hours, with 24 hours having the highest number of Bysl positive cells observed (Figures 2, 3, 6, 7, and 11). The scale bar in each image represents 20 μm .

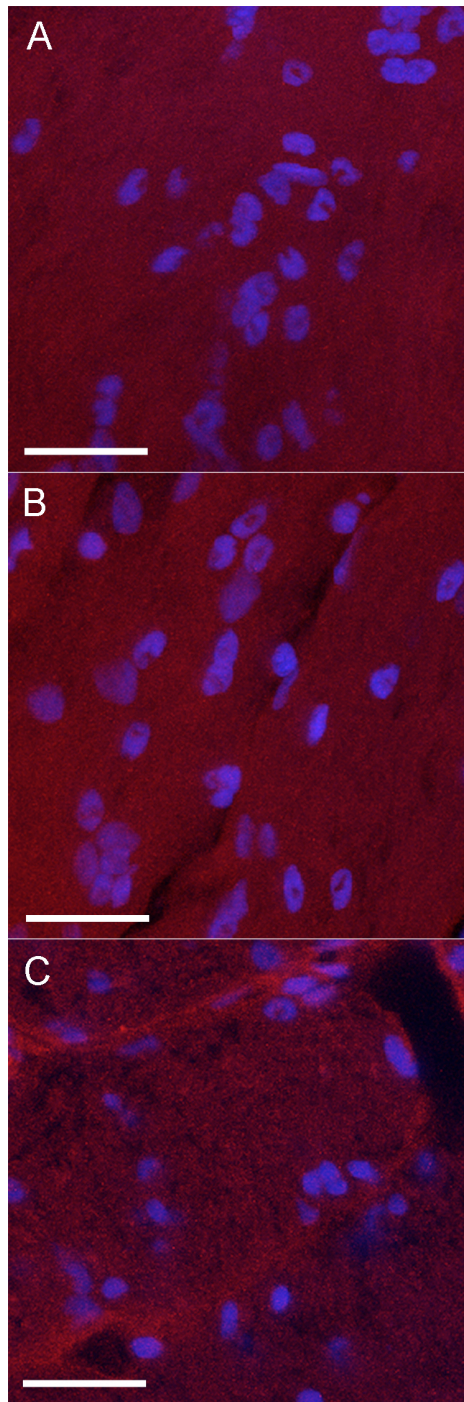


Figure 10: Bysl does not appear to follow a diurnal pattern of expression in the optic nerve of zebrafish. Confocal images of the optic nerve of zebrafish sacrificed at the same (A) 12 (B) 18 and (C) 24 hour time points as injured fish (Figure 9). Each image presented is a z-projection of 20 optical sections 0.5 μm thick obtained using a 60x oil-immersion objective (NA 1.4). Bysl did not appear to label any nucleated cells in uninjured fish at any time point. This result suggests that the anti-bystin immunolabeling seen within 12 hours following nerve lesion is not attributable to a diurnal pattern of expression. Scale bars in each image represent 20 μm .

Activating transcription factor 3 (Atf3), a member of the cAMP-response element binding protein family, has been previously observed to be upregulated in response to various stressors in nervous tissue. In order to elucidate if reactive astrocytes were responsible for the elevated Atf3 expression previously observed in the zebrafish optic nerve, a double immunolabeling experiment was performed using anti-ATF3 and anti-bystin antibodies on injured optic nerve 24 hours after nerve lesion (Figure 11). Atf3 and Bysl labeling colocalized in the cytoplasm of the same cells along the periphery of fascicles of injured nerves. Atf3 labeling was also observed in Bysl-negative cells within fascicles and throughout the entire length of the optic nerve.

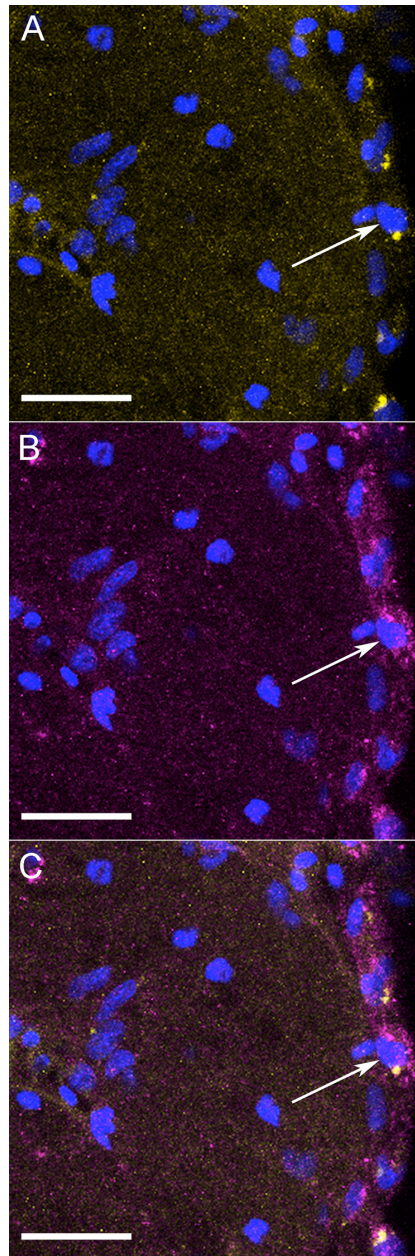


Figure 11: Byst1 colocalizes with Atf3 in reactive astrocytes of the optic nerve of zebrafish after nerve lesion. Confocal images of zebrafish optic nerve obtained 24 hours post-injury. Each image is a z-projection of 20 optical sections 0.5 μm thick obtained using a 60x oil-immersion objective (NA 1.4). Nuclei appear blue in all images. A, B, and C are identical and show an example of an optic nerve astrocyte (arrow). In A, yellow indicates Byst1 localization determined by direct immunofluorescence; in B, magenta indicates anti-ATF3, and C is A and B merged. The colocalization of Byst1 with Atf3 identifies that reactive astrocytes are, in part, responsible for the elevated expression of Atf3 in the optic nerve following nerve lesion (Saul *et al.*, 2010). Atf3 immunolabeling can also be seen in Byst1-negative cells, possibly in the axoplasm of RGS axons (Neve *et al.*, 2011). Scale bars in each image represent 20 μm .

CHAPTER IV

DISCUSSION

In this project I aimed to elucidate whether the astrocytes in the zebrafish optic nerve undergo a reactive transition following nerve lesion. Bystin has recently been proposed as a novel marker for reactive astrocytes *in vivo* (Sheng *et al.*, 2004) and *in vitro* (Sheng *et al.*, 2004; Fang *et al.*, 2008). Elevated bystin expression was detected immunohistochemically and by RT-PCR analysis after 6-hydrodopamine lesion and stab lesion of the nigrostriatum and cerebral cortex of adult rats, respectively. This up-regulation of bystin in reactive astrocytes is more dramatic than that of GFAP, the traditional marker for reactivity, since its expression is minimal in quiescent cells (Sheng *et al.*, 2004). In addition, studies performed on primary cultures of astrocytes from neonatal rats show bystin expression is more sensitive than GFAP to forskolin (Sheng *et al.*, 2004) and hypoxic and ischemic conditions (Fang *et al.*, 2008), allowing reactive astrocytes to be detected earlier after insult. Using an antibody raised against human bystin, I was able to identify hypertrophic astrocytes in the periphery of fascicles of the optic nerve of zebrafish after nerve lesion. These cells have morphological characteristics consistent with reticular astrocytes previously described to form a sheet-like meshwork in which cytokeratin bundles are linked by desmosomes in the periphery of fascicles of the optic nerve (Maggs and Scholes, 1990). The epitope recognized by the

anti-human bystin antibody used in this study (clone S20) had a 90% identity to the homologous epitope of zebrafish Bysl, making it an appropriate antibody to detect changes in Bysl expression following injury. The correlation between hypertrophy and increased Bysl expression supports my hypothesis that astrocytes of the zebrafish optic nerve transition from a quiescent to a reactive state following nerve lesion.

The astrocytes in the optic nerve of fish and some amphibians express cytokeratins as their intermediate filament (Markl and Franke, 1988; Rungger-Brandle *et al.*, 1989; Conrad *et al.*, 1998,). A possible exception is goldfish, in which GFAP positive astrocytes were detected using anti-GFAP antibodies both proximal and distal to an optic nerve crush. The crush site itself was void of GFAP positive cells, however, and there was no mention of analysis performed to determine if the GFAP positive astrocytes had become reactive following nerve injury (Nona *et al.*, 2000). Cytokeratin expressing astrocytes differ from the GFAP expressing astrocytes found in most amniotic organisms in that they do not appear to increase intermediate filament expression following nerve insult (Koke *et al.*, 2010), a characteristic that is a standard for identifying reactivity (Silver and Miller, 2004).

Bysl seemed to completely co-localize with cytokeratin in injured nerves 24 hours after nerve lesion. This labeling was absent in the contralateral nerve of injured fish and both optic nerves of uninjured zebrafish sacrificed at the same, midday time point. Cytokeratin expression was consistent with previously described patterns of immunolabeling (Conrad *et al.*, 1998), and there was no observable difference in the degree of labeling between the injured and contralateral nerves. Cytokeratin did, however, label cells in the injured nerve with no detectable Bysl expression. This

observation was not surprising, however, since it is not likely that an injury would induce every astrocyte in the optic nerve to undergo a reactive transition. In addition, anti-bystin antibodies failed to label oligodendrocytes as detected by EGFP expression in *olig2:egfp* transgenic zebrafish. While I cannot currently rule out the possibility that anti-bystin is also labeling microglia, these findings strongly suggest that anti-bystin is labeling astrocytes of the injured optic nerve.

Established characteristics of reactive astrocytes include hypertrophy and hyperplasia, with an accompanying enlargement of astrocyte nuclei (Diemer, 1977; Fraser *et al.*, 2004). While the term hypertrophy suggest a general increase in cell size, a recent study suggest that the hypertrophic phenotype of reactive astrocytes is limited to an enlargement of cytoplasmic processes. The overall cell body size, surface area, and interdigitation of cytoplasmic processes of quiescent and reactive astrocytes are similar in the hippocampus and cerebral cortex of normal and brain lesioned mice (Wilhelmsson *et al.*, 2006). In order to determine if Bysl positive cells of the injured nerve display a hypertrophic phenotype, the size of astrocytes nuclei were compared between the injured and contralateral nerves (Pekny *et al.*, 2007). The average area of astrocytes nuclei in the injured nerve was significantly larger ($p < 0.01$) than astrocytes from the contralateral nerve. Astrocytes of the uninjured, contralateral nerve were determined by morphological characteristics since Bysl expression was not observed in these cells. The affirmation that Bysl positive astrocytes possess a hypertrophic phenotype further suggests that Bysl expression is a valid marker for astrocytes reactivity in zebrafish.

Bysl expression became apparent within 12 hours following nerve lesion; however, it was only seen in 1 of 5 sections analyzed (representing two fish). The

number of Bysl positive cells increased at 18 hours following nerve lesion and was at its highest of the time points analyzed after 24 hours. Bystin labeling following lesion to the adult rat brain has been reported to persist up to 5 weeks after CNS insult (Sheng *et al.*, 2004). The scarcity of labeling seen in the fish sacrificed 12 hours post injury may indicate Bysl expression is just reaching detectable levels. GFAP expression has been detected as early as 4 hours after CNS injury in mammals (Li *et al.*, 1998); however, many studies do not report an up-regulation of GFAP until at least 24 hours (Hozumi *et al.*, 1990; Herrera *et al.*, 1992; Hausemann *et al.*, 2000).

Beginning from larval development, fish display many functions that follow a diurnal pattern of expression (Ekstrom and Meissl, 1997). Microarray analysis performed on whole eye samples from fish sacrificed at midnight and midday show 44 genes significantly differentially expressed between these two time points. While Bysl was represented on the zebrafish microarray analyzed, these spots were intensity flagged, suggesting inadequate amounts of mRNA was present for reliable detection (Sharma, 2011). In order to determine if the Bysl expression observed at 12 and 18 hours post lesion is due to diurnal changes in expression levels, normal (uninjured) fish were sacrificed at the same 12, 18, and 24 hour time points as their injured counterparts. There was no immunodetectable Bysl expression in any of the uninjured fish analyzed. This finding suggests that the Bysl expression in the injured optic nerve is a direct result of nerve lesion, not a function of a diurnal pattern of expression.

Activating transcription factor 3 (Atf3) is a basic region/leucine zipper (bZIP) containing member of the cAMP-response element binding protein family (Fawcett *et al.*, 1999). Members of the ATF/CREB family of transcription factors can homo- or

heterodimerize with other members of their family or with other bZIP containing transcription factors such as JUN proteins (Veldman *et al.*, 2007). Atf3 has previously been characterized as a stress response gene (Chen *et al.*, 1996) with many characteristics of immediate-early response genes (Wolfgang *et al.*, 1997). In nervous tissue, cerebral ischemia has been shown to induce a biphasic expression of ATF3 (Ohba *et al.*, 2003). Similarly, sciatic nerve injury leads to the up-regulation of ATF3 in glial cells (Hunt *et al.*, 2004). In zebrafish, microarray analysis of retina from optic nerve injured versus sham operated fish revealed a significant up-regulation of *atf3* at 24 and 128 hours following nerve lesion (Saul *et al.*, 2010). The up-regulation of *atf3* mRNA within 3 hours post nerve lesion indicates an earlier activation of its transcription in zebrafish than has been previously reported following spinal cord lesion in rats (Tsujino *et al.*, 2000). In situ hybridization using *atf3*-specific probes revealed elevated expression in the optic nerve following injury; however, the specific cell type responsible for this up-regulation had not been determined (Saul *et al.*, 2010). I was able to determine that reactive astrocytes are in part responsible for elevated Atf3 expression following nerve lesion. Atf3 labeling was also observed in Byst-negative cells within fascicles and throughout the entire length of the optic nerve. Immunogold analysis of Atf3 expression revealed elevated Atf3 expression in the axoplasm of RGC axons after nerve injury (Neve *et al.*, 2011). This pattern of expression may mimic the expression pattern of the transcription factor Engrailed in regenerating RGC axons (Di Nardo *et al.*, 2007). Atf3 labeling in reactive astrocytes seemed to be predominantly located in the cytoplasm, suggesting it may have a cytoplasmic function in addition to regulating gene transcription.

Role of Reactive Astrocytes in Wound Repair

In mammals, astrocytes become reactive in response to all forms of CNS injury and many disease processes; however, the exact mechanism that leads to a reactive phenotype remains unclear. Reactive astrocytes migrate to and become the main cellular inhabitant of lesion sites in the CNS, forming a glial scar that serves as a cellular barrier surrounding the immediate penumbra of the lesion. The formation of a glial scar and astrocyte reactivity in response to CNS insult has been the focus of many studies involving nerve regeneration, with evidence to suggest these processes have both inhibitory and protective effects on axonal repair.

When regenerating axons begin to sprout into a glial scar, dystrophic end bulbs begin to form around neurite growth cones and sprouting halts (see Silver and Miller, 2004). If neurites are unable to surpass the glial scar, regenerating axons fail to reach their synaptic targets and a functional recovery of the damaged nerve is not obtained. Interestingly, end bulb formation does not retard the ability of axons to return to a regenerative state, demonstrated by the ability of injured axons in the spinal cord to regenerate into peripheral nerve grafts weeks after stagnation in the environment of glial scars (Houle, 1991; Li and Raisman, 1995). This suggests that at least a subset of neurons in the CNS are capable of long distance regeneration, and it is extrinsic factors, or the lack thereof, in the CNS that inhibits axon repair. Recent studies on nerve regeneration in mammals have also identified factors endogenous to neurons that prevent axonal regrowth. Deletion of PTEN, a protein that regulates molecular pathways (P13K/mTOR) that control cell growth and size, induces extensive axon regeneration after optic nerve crush in mice. The mTOR pathway is suppressed by PTEN in

axotomized mouse neurons, possibly limiting the protein synthesis required for sustained axon regeneration (Park *et al.*, 2008). Thus, understanding both the endogenous factors of neurons and the molecular environment around CNS lesion sites is essential to the development of treatment methods following CNS injury.

Proteoglycans produced by reactive astrocytes, particularly chondroitin sulfate proteoglycans (CSPG), have been shown to impede neurite extension *in vivo* (Pindzola *et al.*, 1993) and *in vitro* (McKeon *et al.*, 1991). Neurites cultured on alternating bands of laminin and chondroitin sulfate proteoglycan show robust outgrowth on laminin, but turn away sharply at the interface with chondroitin sulfate proteoglycans as a result of selective retraction of filopodia in contact with CSPG (Snow *et al.*, 1990; Hynds *et al.*, 1999). Using a nitrocellulose membrane implantation, the cellular components of the glial scar were explanted from the cerebral cortex of adult rats and treated with chondroitinase to remove the glycosaminoglycan side chains from chondroitin sulfate proteoglycan. Retinal ganglion cells cultured on scar explants were only able to extend neurites for long distances after enzymatic breakdown of chondroitin sulfate (McKeon *et al.*, 1995).

In addition to proteoglycans, reactive astrocytes also upregulate the expression of ephrin-B2 at lesion sites of the CNS (Du *et al.*, 2007). While this molecule alone can impede axon regeneration by elevating intracellular calcium levels in regenerating neurons, it also leads to the increased expression of EPHB2 in fibroblasts (Du *et al.*, 2007). This pattern of expression signals a cell-type segregation of reactive astrocytes and fibroblasts, creating alternating bands of these two cell types characteristic of the glial scar (Bundeson *et al.*, 2003). While the formation of this network is not greatly

detrimental to axon regeneration, fibroblasts of the glial scar have been shown to secrete semaphorin 3 (SEMA3). This protein acts as a chemorepellant of sprouting neurites through its high-affinity receptor neuropilin1, creating an exclusion zone in the penumbra of the nerve lesion (Pasterkamp *et al.*, 1999; De Winter *et al.*, 2002). Oligodendrocytes have also been shown to impede nerve regeneration, causing growth cones to collapse when they come in contact with cell membrane of oligodendrocytes or their myelin products (Kartje *et al.*, 1999). The growth cone collapse is different than what is seen as a result of contact with proteoglycans. During collapse, the growth cone arrests, collapses, and often retracts.

There is an increasing amount of evidence that suggests that reactive astrocytes and glial scar formation have protective effects following nerve lesion. When the ability of astrocytes to undergo a reactive transition is attenuated, there is an increase in the amount of damaged tissue surrounding CNS lesions. This phenomenon has been demonstrated in transgenic mice expressing herpes simplex virus thymidine kinase (HSV-TK) under the control of a GFAP promoter that are then treated with ganciclovir (Bush *et al.*, 1999; Faulkner *et al.*, 2004), causing astrocytes to die. The resulting inhibition of glial scar formation leads to the spread of inflammation over areas larger than what is seen in wild type mice, detected by increases in CD45 immunoreactivity of inflammatory cells surrounding the nerve lesion (Faulkner *et al.*, 2004). This occurrence is believed to be attributable to the inability of attenuated astrocytes to repair the blood brain barrier, allowing inflammatory cells to invade injured neural tissue. This surmise is supported by the ability of grafted nontransgenic astrocytes to repair blood brain barrier function, with an accompanying observation that the ablation of reactive astrocytes

results in an increase in the amount of local tissue edema compared to control mice (Bush *et al.*, 1999). The ablation of reactive astrocytes after nerve lesion also leads to an increase in the death of both neurons and oligodendrocytes and an increase in demyelination (Bush *et al.*, 1999; Faulkner *et al.*, 2004). Increased cell death is not a result of increased inflammation, since treatment with lipopolysaccharide fails to elicit a similar pattern of cell death (Faulkner *et al.*, 2004). Instead, it is believed that the neuronal cell death in HSV-TK transgenic mice is a result of an accumulation of glutamate. This was confirmed by the ability of memantine, an N-methyl-D-aspartic acid receptor antagonist, to reduce the amount of glutamate-mediated excitotoxicity following nerve lesion (Bush *et al.*, 1999). In similar studies, mutant mice carrying a null mutation for GFAP, vimentin, or both were used to examine the consequences of those mutations on nerve repair (Wilhelmsson *et al.*, 2004; Li *et al.*, 2008). The GFAP/vimentin deficient mice displayed an attenuated ability to form a glial scar, leading to a significant increase of infarct size after cortex lesion (Wilhelmsson *et al.*, 2004) and induction of ischemia (Li *et al.*, 2008). While the elimination of scar formation initially results in an increase in synaptic loss, axons were able to regenerate through the enlarged infarct and complete synaptic regeneration (Wilhelmsson *et al.*, 2004).

Endothelin B receptor (ET_RB) is typically upregulated by reactive astrocytes following CNS injury (Peters *et al.*, 2003). ET_RB upregulation was not observed in astrocytes with attenuated reactivity after either cortex lesion or induction of ischemia (Li *et al.*, 2008). Failure to upregulate ET_RB may have a consequence in the ability of this receptor to effectively mediate gap junction communication in GFAP/vimentin deficient mice, possibly resulting in the observed increase in synaptic deterioration and infarct size

(Li *et al.*, 2008). Similarly, deletion of the protein signal transducer and activator of transcription 3 (STAT3) in mice resulted in astrocytes with an attenuated ability to migrate towards and accumulate around a spinal cord lesion (Okada *et al.*, 2006). This deficiency led to an increase in inflammation, demyelination, and severe motor deficits. Deletion of the inhibitor of STAT3, cytokine signaling 3 (Soc3), led to an increase in the phosphorylation of STAT3 following spinal cord lesion compared to wildtype mice, resulting in less extensive cell death and an increase in motor function compared to wild type mice (Okada *et al.*, 2006). The findings of these studies suggest that reactive astrocytes may initially have a positive role following CNS injury; however, their prolonged presence in the glial scar may also pose an obstacle at a later stage (Li *et al.*, 2008). Understanding the cascade of molecular signals responsible for this duality is pertinent for the development of novel treatment methods to promote axon regeneration in the CNS.

Conclusions and Future Directions.

While elucidating why there is a difference between mammals and fish with respect to the regenerative capacity of nervous tissue is outside of the scope of this project, I was able to determine that astrocytes of fish undergo a reactive transition following nerve lesion. The findings of this study demonstrate that antibodies raised against bystin of human origin (clone S20 in particular) are suitable tools for identifying reactive astrocytes in zebrafish; similar to what has previously been reported in rats (Sheng *et al.*, 2004; Fang *et al.*, 2008). Using Bystl expression as a marker of reactivity, I observed that Atf3 is expressed by reactive astrocytes following nerve injury. The up-regulation of Atf3 by reactive astrocytes may suggest its role in the transition from a

quiescent to a reactive state; however, further investigation is needed to confirm this hypothesis. I also cannot conclusively rule out microglia as a possible source of Bysl expression, and future studies will seek to resolve whether both astrocytes and microglia express Bysl in response to injury. There is a limited repertoire of microglial markers available for fish compared to what has been described in mammals. Monocyte-derived cells have been identified by positive immunoreactivity to OX-42 antibodies, directed against the complement component receptor C3bi, and Fl.1 antibodies, homologous to CD45, in goldfish and cichlids, respectively (Dowding *et al.*, 1991; Battisti *et al.*, 1995). Lectins derived from tomato (*Lycopersicon esculentum*) have affinity for poly-N-acetyl lactosamine sugar residues present on both amoeboid and ramified microglial cells (Cuoghi and Mola, 2007). This protein has been observed to label microglia in normal and injured fish retina, optic nerve, and optic tectum (Velasco *et al.*, 1995), suggesting lectin is a feasible marker to elucidate Bysl expression in microglia following optic nerve lesion. The anti-bystin immunoreactivity seen in this study seemed to completely colocalize with cytokeratin. Retinal microglia in rats have been shown to express vimentin and nestin, not cytokeratin, as their intermediate filaments (Wohl *et al.*, 2011). In addition, anti-bystin failed to label microglia, identified by CD11b immunoreactivity, after lesion of the nigrostriatum and cortex of adult rats (Sheng *et al.*, 2004). If microglia of fish and mammals share similar patterns of intermediate filament expression and response to injury, these observations suggest microglia are not responsible for the elevated Bysl expression in the zebrafish optic nerve following nerve lesion.

The identification of Bysl-positive, reactive astrocytes following lesion to the optic nerve supports using zebrafish as a model organism with relevance to human health.

Future studies may be directed to determine if the molecular mechanisms responsible for the transition to a reactive phenotype are similar between astrocytes of fish and mammals. In primary cultures of astrocytes derived from neonatal rats, interleukin- β (IL- β) and nerve growth factor (NGF) induced an upregulation of bystin and GFAP expression in astrocytes (Sheng *et al.*, 2004). The expression of cytokines, including IL- β , interferon- γ (If- γ) and tumor necrosis factor- α (TNF- α), have been correlated with nerve lesion, associated with elevated levels of the endotoxin lipopolysaccharide (Lieberman *et al.*, 1989). In addition, IL- β and TNF- α can regulate secretion of NGF in reactive astrocytes in rats (Wu *et al.*, 1998; Juric and Carman-Krzan, 2001). It would be interesting to investigate if these various cytokines and NGF can stimulate astrocytes to undergo a reactive transition in fish similar to what is observed in rats. Also, a plant-derived activator of adenylyl cycles, forskolin, has been used to induce reactivity of astrocytes *in vitro* (Fang *et al.*, 2004; Tramontina *et al.*, 2007; Juric *et al.*, 2011), suggesting cAMP acts as a second messenger in the pathway to reactivity. Preliminary analysis performed by Sarah Kane at Texas State University suggests intracellular cAMP acts through PKA and EPAC to induce reactivity in F98 cells, a cell line that has been used to model astrocytes. Activation of these macromolecules may shed light on whether astrocytes in the fish optic nerve share a common mechanism of activation with mammalian astrocytes. These studies could be performed using a Gelfoam delivery system similar to what has been used for morpholino transfection to knockdown KLF6a and KLF7a in the zebrafish optic nerve (Veldman *et al.*, 2007).

This study was the first to observe reactive astrocytes following nerve lesion in a zebrafish model. While this observation is valid on its own, finding a correlation

between the mechanisms leading to reactivity in zebrafish and mammals would enhance the relevance of studies comparing fish and mammals with respect to their regenerative capabilities of the CNS.

APPENDIX

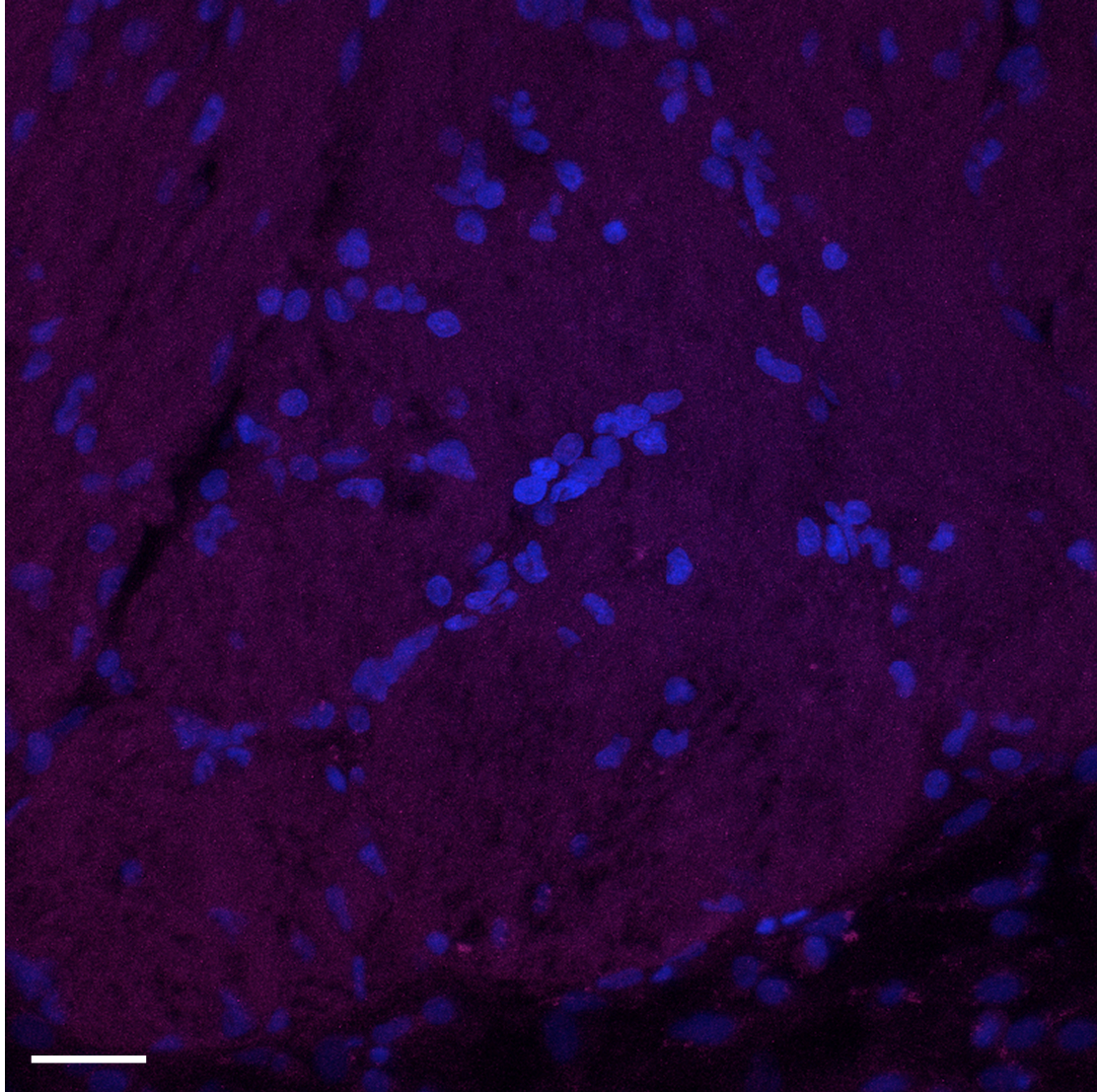


Figure 12: Cytokeratin no primary control. Confocal image of an injured optic nerve labeled the sheep anti-mouse IgG-Cy5 secondary antibody used to detect the anti-cytokeratin primary antibody. This image is a z-projection of 20 optical sections each 0.5 μm thick obtained using a 60x oil immersion objective with a numerical aperture of 1.4. Nuclei appear blue in this image. No labeling attributable to sheep anti-mouse IgG Cy5 secondary antibody is observed in the absence of primary antibody.

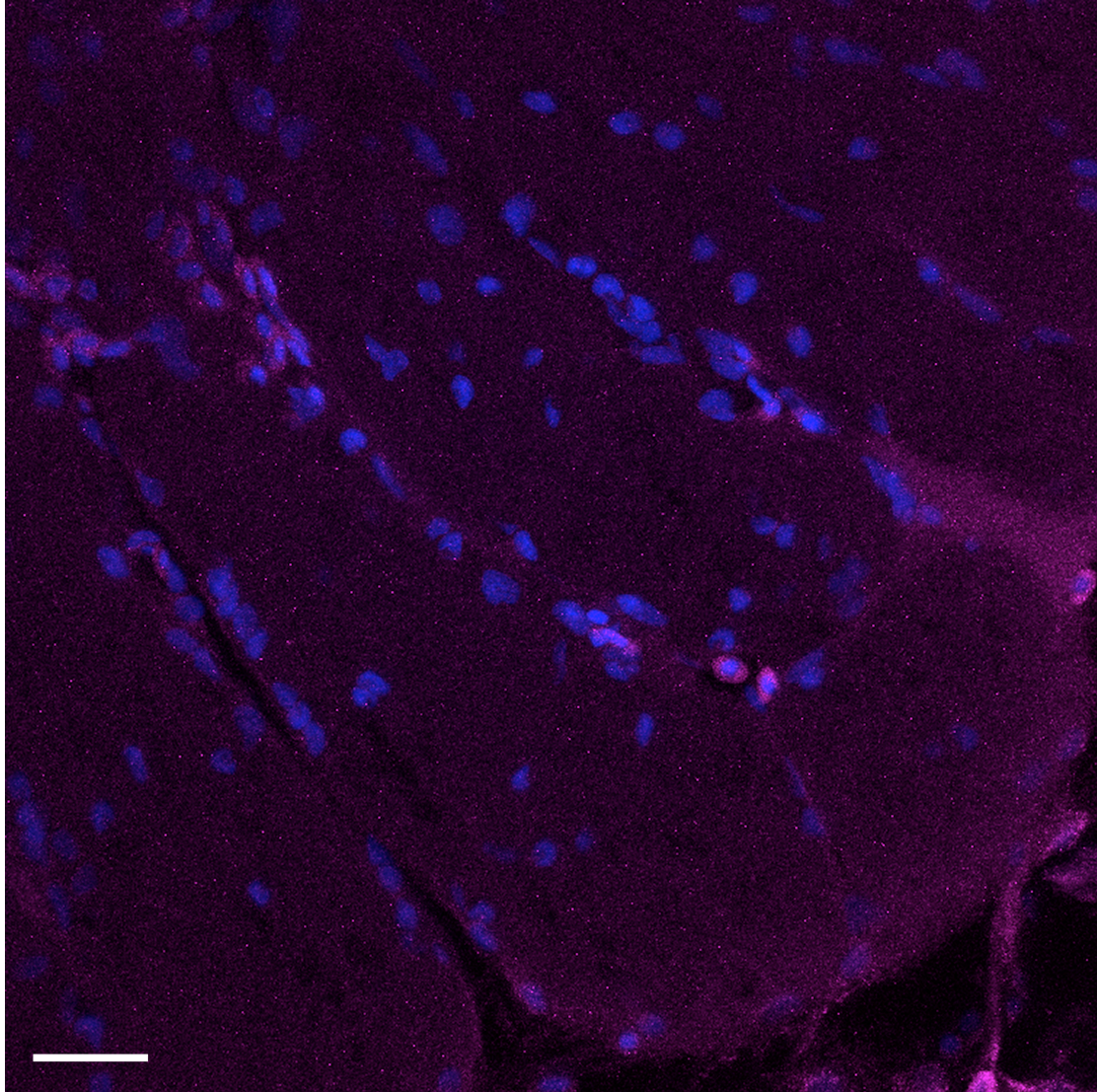


Figure 13: Atf3 no primary control. Confocal image of an injured optic nerve labeled with the chicken anti-rabbit IgG-AlexaFluor647 secondary antibody used to detect the anti-ATF3 primary antibody. This image is a z-projection of 20 optical sections each 0.5 μm thick obtained using a 60x oil immersion objective (NA 1.4). Nuclei appear blue in this image. No labeling attributable to chicken anti-rabbit IgG-AlexaFluor647 secondary antibody is observed in the absence of primary antibody.

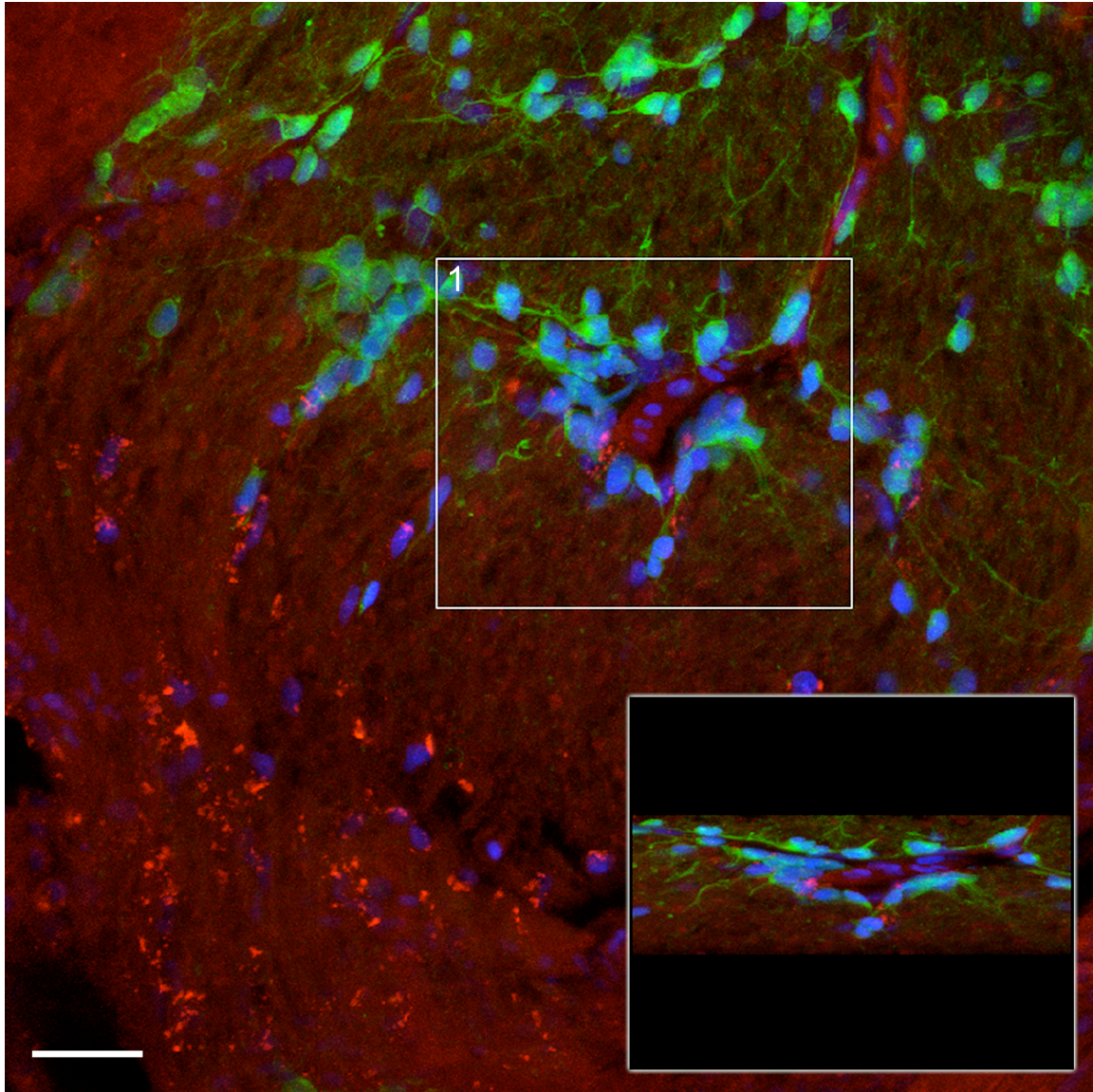


Figure 14: Three dimensional analysis of Bysl labeling in a *tg(olig2:EGFP)* zebrafish. Confocal image of an injured optic nerve of a transgenic *olig2:efgp* zebrafish 24 hours after nerve lesion. This image is identical to the image presented in Figure 7. The insert in this image is the area identified by box 1 rotated along the x-axis to depict the EGFP expression and Bysl labeling in the z-dimension. The cells that appear to present Olig2 and Bysl colocalization in the 2D z-projection in box 1 are actually different cells occupying the same (x,y) coordinates in different z-planes. This analysis further demonstrates that Bysl is not being expressed by oligodendrocytes in the injured zebrafish optic nerve.

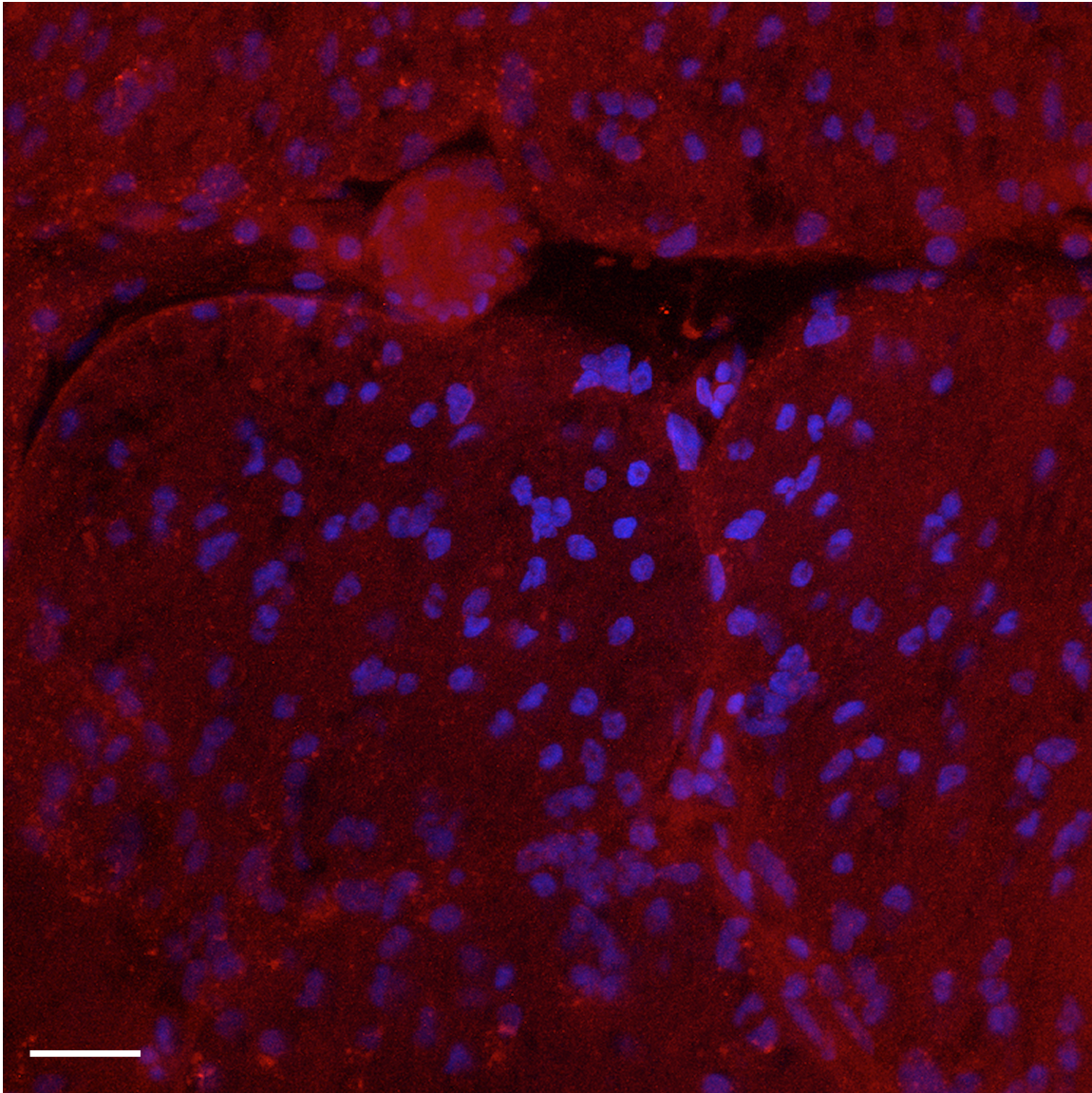


Figure 15: Goat IgG Isotype Control. Confocal image of an injured optic nerve labeled with goat anti-mouse IgG conjugated to Texas Red to serve as a negative control for Bystin labeling. This image is a z-projection of 20 optical sections each 0.5 μm thick obtained using a 60x oil immersion objective (NA 1.4). Nuclei appear blue in this image. The concentration of antibody used and microscopy settings are identical to what was used to collect the image presented in Figure 3. The labeling pattern and intensity observed using this goat IgG is different from what has been observed using the directly conjugated anti-bystin antibody, suggesting the pattern of bystin expression observed at 24 hours is not attributable to non-specific antibody binding

REFERENCES

- Barresi, M. J., Burton, S., Dipietrantonio, K., Amsterdam, A., Hopkins, N., & Karlstrom, R. O. (2010). Essential genes for astroglial development and axon pathfinding during zebrafish embryogenesis. *Dev Dyn*, 239(10), 2603-2618.
- Battisti, W. P., Wang, J., Bozek, K., & Murray, M. (1995). Macrophages, microglia, and astrocytes are rapidly activated after crush injury of the goldfish optic nerve: a light and electron microscopic analysis. *J Comp Neurol*, 354(2), 306-320.
- Becker, C. G., & Becker, T. (2002). Repellent guidance of regenerating optic axons by chondroitin sulfate glycosaminoglycans in zebrafish. *J Neurosci*, 22(3), 842-853.
- Becker, T., Bernhardt, R. R., Reinhard, E., Wullimann, M. F., Tongiorgi, E., & Schachner, M. (1998). Readiness of zebrafish brain neurons to regenerate a spinal axon correlates with differential expression of specific cell recognition molecules. *J Neurosci*, 18(15), 5789-5803.
- Bernhardt, R. R., Tongiorgi, E., Anzini, P., & Schachner, M. (1996). Increased expression of specific recognition molecules by retinal ganglion cells and by optic pathway glia accompanies the successful regeneration of retinal axons in adult zebrafish. *J Comp Neurol*, 376(2), 253-264.
- Bundesen, L. Q., Scheel, T. A., Bregman, B. S., & Kromer, L. F. (2003). Ephrin-B2 and EphB2 regulation of astrocyte-meningeal fibroblast interactions in response to spinal cord lesions in adult rats. *J Neurosci*, 23(21), 7789-7800.
- Bush, T. G., Puvanachandra, N., Horner, C. H., Polito, A., Ostensfeld, T., Svendsen, C. N. et al. (1999). Leukocyte infiltration, neuronal degeneration, and neurite outgrowth after ablation of scar-forming, reactive astrocytes in adult transgenic mice. *Neuron*, 23(2), 297-308.
- Chen, B. P., Wolfgang, C. D., & Hai, T. (1996). Analysis of ATF3, a transcription factor induced by physiological stresses and modulated by gadd153/Chop10. *Mol Cell Biol*, 16(3), 1157-1168.

- Cohen, I., Shani, Y., & Schwartz, M. (1993). Cloning and characteristics of fish glial fibrillary acidic protein: implications for optic nerve regeneration. *J Comp Neurol*, 334(3), 431-443.
- Conrad, M., Lemb, K., Schubert, T., & Markl, J. (1998). Biochemical identification and tissue-specific expression patterns of keratins in the zebrafish *Danio rerio*. *Cell Tissue Res*, 293(2), 195-205.
- Cuoghi, B., & Mola, L. (2007). Microglia of teleosts: facing a challenge in neurobiology. *Eur J Histochem*, 51(4), 231-240.
- De Winter, F., Oudega, M., Lankhorst, A. J., Hamers, F. P., Blits, B., Ruitenberg, M. J. et al. (2002). Injury-induced class 3 semaphorin expression in the rat spinal cord. *Exp Neurol*, 175(1), 61-75.
- Di Nardo, A. A., Nedelec, S., Trembleau, A., Volovitch, M., Prochiantz, A., & Montesinos, M. L. (2007). Dendritic localization and activity-dependent translation of Engrailed1 transcription factor. *Mol Cell Neurosci*, 35(2), 230-236.
- Diemer, N. H. (1977). Glial and neuronal alteration in the corpus striatum or rats with CCl₄-induced liver disease. A quantitative morphological study using an electronic image analyzer. *Acta Neurol Scand*, 55(1), 16-32.
- Dowding, A. J., Maggs, A., & Scholes, J. (1991). Diversity amongst the microglia in growing and regenerating fish CNS: immunohistochemical characterization using FL1, an anti-macrophage monoclonal antibody. *Glia*, 4(4), 345-364.
- Du, J., Tran, T., Fu, C., & Sretavan, D. W. (2007). Upregulation of EphB2 and ephrin-B2 at the optic nerve head of DBA/2J glaucomatous mice coincides with axon loss. *Invest Ophthalmol Vis Sci*, 48(12), 5567-5581.
- Ekstrom, P., & Meissl, H. (1997). The pineal organ of teleost fishes. *Trends in Endocrinology and Metabolism*, 18, 81-88.
- Fang, D., Li, Z., Zhong-ming, Q., Mei, W. X., Ho, Y. W., Yuan, X. W. et al. (2008). Expression of bystin in reactive astrocytes induced by ischemia/reperfusion and chemical hypoxia in vitro. *Biochim Biophys Acta*, 1782(11), 658-663.
- Faulkner, J. R., Herrmann, J. E., Woo, M. J., Tansey, K. E., Doan, N. B., & Sofroniew, M. V. (2004). Reactive astrocytes protect tissue and preserve function after spinal cord injury. *J Neurosci*, 24(9), 2143-2155.

- Fawcett, T. W., Martindale, J. L., Guyton, K. Z., Hai, T., & Holbrook, N. J. (1999). Complexes containing activating transcription factor (ATF)/cAMP-responsive-element-binding protein (CREB) interact with the CCAAT/enhancer-binding protein (C/EBP)-ATF composite site to regulate Gadd153 expression during the stress response. *Biochem J*, 339(Pt 1), 135-141.
- Fraser, M. M., Zhu, X., Kwon, C. H., Uhlmann, E. J., Gutmann, D. H., & Baker, S. J. (2004). Pten loss causes hypertrophy and increased proliferation of astrocytes in vivo. *Cancer Res*, 64(21), 7773-7779.
- García, D. M., & Koke, J. R. (2009). Astrocytes as gate-keepers in optic nerve regeneration--a mini-review. *Comp Biochem Physiol A Mol Integr Physiol*, 152(2), 135-138.
- García, D. M., Bauer, H., Dietz, T., Schubert, T., Markl, J., & Schaffeld, M. (2005). Identification of keratins and analysis of their expression in carp and goldfish: comparison with the zebrafish and trout keratin catalog. *Cell Tissue Res*, 322(2), 245-256.
- Hausmann, R., Riess, R., Fieguth, A., & Betz, P. (2000). Immunohistochemical investigations on the course of astroglial GFAP expression following human brain injury. *Int J Legal Med*, 113(2), 70-75.
- Herrera, D. G., & Cuello, A. C. (1992). Glial fibrillary acidic protein immunoreactivity following cortical devascularizing lesion. *Neuroscience*, 49(4), 781-791.
- Houle, J. D. (1991). Demonstration of the potential for chronically injured neurons to regenerate axons into intraspinal peripheral nerve grafts. *Exp Neurol*, 113(1), 1-9.
- Hozumi, I., Chiu, F. C., & Norton, W. T. (1990). Biochemical and immunocytochemical changes in glial fibrillary acidic protein after stab wounds. *Brain Res*, 524(1), 64-71.
- Hunt, D., Hossain-Ibrahim, K., Mason, M. R., Coffin, R. S., Lieberman, A. R., Winterbottom, J. et al. (2004). ATF3 upregulation in glia during Wallerian degeneration: differential expression in peripheral nerves and CNS white matter. *BMC Neurosci*, 5, 9.
- Hynds, D. L., & Snow, D. M. (1999). Neurite outgrowth inhibition by chondroitin sulfate proteoglycan: stalling/stopping exceeds turning in human neuroblastoma growth cones. *Exp Neurol*, 160(1), 244-255.

- Jackson ImmunoResearch (2011). Retrieved November 10, 2011, from <http://www.jacksonimmuno.com/technical/select.asp>
- Juric, D. M., & Carman-Krzan, M. (2001). Interleukin-1 beta, but not IL-1 alpha, mediates nerve growth factor secretion from rat astrocytes via type I IL-1 receptor. *Int J Dev Neurosci*, 19(7), 675-683.
- Juric, D. M., Mele, T., & Carman-Krzan, M. (2011). Involvement of histaminergic receptor mechanisms in the stimulation of NT-3 synthesis in astrocytes. *Neuropharmacology*, 60(7-8), 1309-1317.
- Kartje, G. L., Schulz, M. K., Lopez-Yunez, A., Schnell, L., & Schwab, M. E. (1999). Corticostriatal plasticity is restricted by myelin-associated neurite growth inhibitors in the adult rat. *Ann Neurol*, 45(6), 778-786.
- Koke, J. R., Mosier, A. L., & García, D. M. (2010). Intermediate filaments of zebrafish retinal and optic nerve astrocytes and Muller glia: differential distribution of cytokeratin and GFAP. *BMC Res Notes*, 3, 50.
- Levine, J. M., Reynolds, R., & Fawcett, J. W. (2001). The oligodendrocyte precursor cell in health and disease. *Trends Neurosci*, 24(1), 39-47.
- Li, L., Lundkvist, A., Andersson, D., Wilhelmsson, U., Nagai, N., Pardo, A. C. et al. (2008). Protective role of reactive astrocytes in brain ischemia. *J Cereb Blood Flow Metab*, 28(3), 468-481.
- Li, R., Fujitani, N., Jia, J. T., & Kimura, H. (1998). Immunohistochemical indicators of early brain injury: an experimental study using the fluid-percussion model in cats. *Am J Forensic Med Pathol*, 19(2), 129-136.
- Li, Y., & Raisman, G. (1995). Sprouts from cut corticospinal axons persist in the presence of astrocytic scarring in long-term lesions of the adult rat spinal cord. *Exp Neurol*, 134(1), 102-111.
- Lieberman, A. P., Pitha, P. M., Shin, H. S., & Shin, M. L. (1989). Production of tumor necrosis factor and other cytokines by astrocytes stimulated with lipopolysaccharide or a neurotropic virus. *Proc Natl Acad Sci U S A*, 86(16), 6348-6352.
- Liu, Q., & Londraville, R. L. (2003). Using the adult zebrafish visual system to study cadherin-2 expression during central nervous system regeneration. *Methods Cell Sci*, 25(1-2), 71-78.

- Maggs, A., & Scholes, J. (1990). Reticular astrocytes in the fish optic nerve: macroglia with epithelial characteristics form an axially repeated lacework pattern, to which nodes of Ranvier are apposed. *J Neurosci*, *10*(5), 1600-1614.
- Markl, J., & Franke, W. W. (1988). Localization of cytokeratins in tissues of the rainbow trout: fundamental differences in expression pattern between fish and higher vertebrates. *Differentiation*, *39*(2), 97-122.
- McKeon, R. J., Hoke, A., & Silver, J. (1995). Injury-induced proteoglycans inhibit the potential for laminin-mediated axon growth on astrocytic scars. *Exp Neurol*, *136*(1), 32-43.
- McKeon, R. J., Schreiber, R. C., Rudge, J. S., & Silver, J. (1991). Reduction of neurite outgrowth in a model of glial scarring following CNS injury is correlated with the expression of inhibitory molecules on reactive astrocytes. *J Neurosci*, *11*(11), 3398-3411.
- Neve, L. D., Savage, A. A., Koke, J. R., & García, D. M. (in press). Activating transcription factor 3 and reactive astrocytes following optic nerve injury in zebrafish. *Comp Biochem Physiol C Toxicol Pharmacol*.
- Nona, S. N., Thomlinson, A. M., Bartlett, C. A., & Scholes, J. (2000). Schwann cells in the regenerating fish optic nerve: evidence that CNS axons, not the glia, determine when myelin formation begins. *J Neurocytol*, *29*(4), 285-300.
- Ohba, N., Maeda, M., Nakagomi, S., Muraoka, M., & Kiyama, H. (2003). Biphasic expression of activating transcription factor-3 in neurons after cerebral infarction. *Brain Res Mol Brain Res*, *115*(2), 147-156.
- Okada, S., Nakamura, M., Katoh, H., Miyao, T., Shimazaki, T., Ishii, K. et al. (2006). Conditional ablation of Stat3 or Socs3 discloses a dual role for reactive astrocytes after spinal cord injury. *Nat Med*, *12*(7), 829-834.
- Park, K. K., Liu, K., Hu, Y., Smith, P. D., Wang, C., Cai, B. et al. (2008). Promoting axon regeneration in the adult CNS by modulation of the PTEN/mTOR pathway. *Science*, *322*(5903), 963-966.
- Pasterkamp, R. J., Giger, R. J., Ruitenber, M. J., Holtmaat, A. J., De Wit, J., De Winter, F. et al. (1999). Expression of the gene encoding the chemorepellent semaphorin III is induced in the fibroblast component of neural scar tissue formed following injuries of adult but not neonatal CNS. *Mol Cell Neurosci*, *13*(2), 143-166.

- Pekny, M., Wilhelmsson, U., Bogestal, Y. R., & Pekna, M. (2007). The role of astrocytes and complement system in neural plasticity. *Int Rev Neurobiol*, 82, 95-111.
- Peters, C. M., Rogers, S. D., Pomonis, J. D., Egnaczyk, G. F., Keyser, C. P., Schmidt, J. A. et al. (2003). Endothelin receptor expression in the normal and injured spinal cord: potential involvement in injury-induced ischemia and gliosis. *Exp Neurol*, 180(1), 1-13.
- Pindzola, R. R., Doller, C., & Silver, J. (1993). Putative inhibitory extracellular matrix molecules at the dorsal root entry zone of the spinal cord during development and after root and sciatic nerve lesions. *Dev Biol*, 156(1), 34-48.
- Rudge, J. S., & Silver, J. (1990). Inhibition of neurite outgrowth on astroglial scars in vitro. *J Neurosci*, 10(11), 3594-3603.
- Saul, K. E., Koke, J. R., & García, D. M. (2010). Activating transcription factor 3 (ATF3) expression in the neural retina and optic nerve of zebrafish during optic nerve regeneration. *Comp Biochem Physiol A Mol Integr Physiol*, 155(2), 172-182.
- Sharma, S. (2011). Diurnal variation of melatonin receptors in *Danio Rerio* (zebrafish). *Thesis and Dissertations-Biology*, Texas State University-San Marcos.
- Sheng, J., Yang, S., Xu, L., Wu, C., Wu, X., Li, A. et al. (2004). Bystin as a novel marker for reactive astrocytes in the adult rat brain following injury. *Eur J Neurosci*, 20(4), 873-884.
- Silver, J., & Miller, J. H. (2004). Regeneration beyond the glial scar. *Nat Rev Neurosci*, 5(2), 146-156.
- Snow, D. M., Steindler, D. A., & Silver, J. (1990). Molecular and cellular characterization of the glial roof plate of the spinal cord and optic tectum: a possible role for a proteoglycan in the development of an axon barrier. *Dev Biol*, 138(2), 359-376.
- Sofroniew, M. V., & Vinters, H. V. (2010). Astrocytes: biology and pathology. *Acta Neuropathol*, 119(1), 7-35.
- Stenkamp, D. L. (2007). Neurogenesis in the fish retina. *Int Rev Cytol*, 259, 173-224.
- Suzuki, N., Nakayama, J., Shih, I. M., Aoki, D., Nozawa, S., & Fukuda, M. N. (1999). Expression of trophinin, tasin, and bystin by trophoblast and endometrial cells in human placenta. *Biol Reprod*, 60(3), 621-627.

- Tan, A., Zhang, W., Uhgrin, Y., Chen, Z., & Levine, J. M. (2004). NG2 at the glial scar: a molecular barrier to nerve regeneration. *J Anat* 204(6), 519-520
- Tramontina, F., Leite, M. C., Cereser, K., de Souza, D. F., Tramontina, A. C., Nardin, P. et al. (2007). Immunoassay for glial fibrillary acidic protein: antigen recognition is affected by its phosphorylation state. *J Neurosci Methods*, 162(1-2), 282-286.
- Tsujino, H., Kondo, E., Fukuoka, T., Dai, Y., Tokunaga, A., Miki, K. et al. (2000). Activating transcription factor 3 (ATF3) induction by axotomy in sensory and motoneurons: A novel neuronal marker of nerve injury. *Mol Cell Neurosci*, 15(2), 170-182.
- Velasco, A., Caminos, E., Vecino, E., Lara, J. M., & Aijon, J. (1995). Microglia in normal and regenerating visual pathways of the tench (*Tinca tinca* L., 1758; Teleost): a study with tomato lectin. *Brain Res*, 705(1-2), 315-324.
- Veldman, M. B., Bemben, M. A., Thompson, R. C., & Goldman, D. (2007). Gene expression analysis of zebrafish retinal ganglion cells during optic nerve regeneration identifies KLF6a and KLF7a as important regulators of axon regeneration. *Dev Biol*, 312(2), 596-612.
- Wilhelmsson, U., Bushong, E. A., Price, D. L., Smarr, B. L., Phung, V., Terada, M. et al. (2006). Redefining the concept of reactive astrocytes as cells that remain within their unique domains upon reaction to injury. *Proc Natl Acad Sci U S A*, 103(46), 17513-17518.
- Wilhelmsson, U., Li, L., Pekna, M., Berthold, C. H., Blom, S., Eliasson, C. et al. (2004). Absence of glial fibrillary acidic protein and vimentin prevents hypertrophy of astrocytic processes and improves post-traumatic regeneration. *J Neurosci*, 24(21), 5016-5021.
- Wohl, S. G., Schmeer, C. W., Friese, T., Witte, O. W., & Isenmann, S. (2011). In situ dividing and phagocytosing retinal microglia express nestin, vimentin, and NG2 in vivo. *PLoS One*, 6(8), e22408.
- Wolfgang, C. D., Chen, B. P., Martindale, J. L., Holbrook, N. J., & Hai, T. (1997). gadd153/Chop10, a potential target gene of the transcriptional repressor ATF3. *Mol Cell Biol*, 17(11), 6700-6707.
- Wu, V. W., Nishiyama, N., & Schwartz, J. P. (1998). A culture model of reactive astrocytes: increased nerve growth factor synthesis and reexpression of cytokine responsiveness. *J Neurochem*, 71(2), 749-756.

Zhou, Q., Choi, G., & Anderson, D. J. (2001). The bHLH transcription factor Olig2 promotes oligodendrocyte differentiation in collaboration with Nkx2.2. *Neuron*, 31(5), 791-807.

VITA

Luis Daniel Neve was born in Dallas, Texas on May 22, 1987 to Irene E. Neve and Luis F. Neve. He was raised in McAllen, Texas, graduating from McAllen Memorial High School with an interest in biology and mathematics. Luis attended Texas State University-San Marcos from 2005-2009, graduating with a B.S. in Biology. In the fall of that same year, he enrolled as a masters candidate in the Biology Department at Texas State. Luis's thesis research has focused on describing the reactive phenotype of astrocytes in the zebrafish CNS following injury, in attempt to further support using zebrafish as a model organism with relevance to human health. His efforts during his masters career were published in August 2011 in Comparative Biochemistry and Physiology – Part C (DOI: 10.1016/j.cbpc.2011.08.006)

Permanent Address: 2015 Verdin Ave.
McAllen, TX 78504

This thesis was typed by Luis D. Neve.